Radio Observations of the HAARP Summer 2018 Research Campaign
Whitham D. Reeve

1. Introduction

The *High Frequency Active Auroral Research Program* (HAARP) conducted research campaigns during spring and summer 2018. I previously reported my radio observations of the spring campaign in {Reeve18} and will discuss the summer campaign here. As should be well-known by now, HAARP is located in interior Alaska and is used to heat a *spot* in Earth's ionosphere for radio science research purposes. HAARP's core is the Ionospheric Research Instrument (IRI), a transmitter and antenna system (figure 1) capable of transmitting a few gigawatts of effective radiated power into the ionosphere above the HAARP site. Each HAARP research campaign has its own science objectives, and the IRI transmissions are tailored to these objectives. Variables include frequencies, number of active antenna array elements, transmitter powers, modulations and beam pointing angles.

Figure 1 ~ HAARP Ionospheric Research Instrument antenna with collocated transmitters as it appeared on 25 August 2018. It consists of 180 crossed-dipole antennas in a 12 x 15 array but not all antennas are serviceable as of this writing (late 2018) and not all antennas are used in every experiment. The white structures almost hidden by foliage are the transmitter enclosures. Part of the surrounding fence is in the foreground. Image © 2018 W. Reeve

The summer campaign, which ran from 30 July through 1 August, had two main purposes. The first was to create magnetic field-aligned electron density irregularities in the ionosphere, and the second was to modulate the IRI transmissions for a *Weak Signal Propagation Reporter* (WSPR) beacon test. Instead of observing these experiments for science purposes, I was interested in the propagation and receiver technical aspects including

the software defined radio (SDR) receiver setups and the Long Wavelength Array (LWA) antenna performance at Cohoe Radio Observatory with respect to HAARP.

All times and dates in this paper are Coordinated Universal Time (UTC) unless noted otherwise. Additional information on the HAARP IRI and related diagnostic instruments can be found in {Reeve16} and {Reeve17}, respectively.

---

2. Phenomena

Although I did not observe the HAARP transmissions for science purposes, I will briefly discuss the science aspects of the research campaign in this section for reference and because they are interesting. The receiver, antenna and software setups described in this paper may be reused to receive any HAARP transmissions but additional equipment or software is required to observe some of the described phenomena because they involve different frequencies or require additional software.

When energy is added to the F-region of the ionosphere near the location of peak electron density, the electron cloud becomes striated with local rod-like enhanced density regions that are aligned with the magnetic field (figure 2). The striated regions can directionally reflect or randomly scatter radio waves at frequencies from HF to UHF on a communications link or modify signals passing through them. The phenomenon is called *field aligned irregularities scattering* (FAIS) and the striated regions are called *field-aligned irregularities* (FAI) or *field-aligned scatterers* (FAS).

Earth's magnetic field lines at the HAARP site have an inclination (angle with respect to the horizon, also called *dip*) of almost 76°. The field lines are within the steerable beam of the IRI and it can be used to artificially produce electron density striations for scattering studies. Although I did not specifically observe this phenomenon during the summer 2018 campaign, I plan to attempt reception of scattering at 440 MHz (70 cm wavelength) in a future campaign.
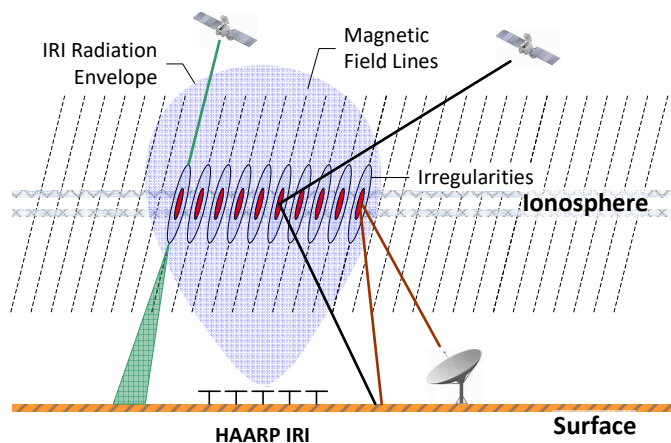
Figure 2 ~ FAIS experiment schematic. The HAARP IRI produces electron density striations (irregularities) in the ionosphere, which scatter man-made ground-ground and ground-space signals. The scattering, which occurs in the HF through UHF frequency bands, can enable or disrupt communication links. Image adapted from {DTIC}

The WSPR aspect of the experiment studied the propagation effects of transmitting large amounts of radio frequency energy at different angles with respect to Earth's magnetic field lines and then seeing what stations received them. WSPR is a very low-speed frequency shift keying modulation protocol (FSK, about 1.5 baud)

{WSPR}. It is designed for weak signal communications between amateur radio operators, such as on Earth-Moon-Earth (EME) paths, and also can be used as a propagation indicator. Participating stations automatically upload reception reports to a central *WSPRnet* database where they may be viewed on a map or data file {WSPRnet}. The automated WSPR beacon network allows inexpensive propagation monitoring from locations around the world and can be used to determine preferential propagation or transmitting directions.

HAARP uses much higher transmitter powers than normal amateur radio communications. HAARP transmissions in the radio amateur band are covered by a Special Temporary Authority (STA) issued by Federal Communications Commission (FCC). Each STA is issued under HAARP's experimental license for call sign WI2XFX. For this experiment, the IRI is modulated according to the WSPR protocol and, thus, citizen scientists with an HF receiver and running the WSPR software are able to participate. I did not have the WSPR software installed so did not directly participate in this part of the experiment.

Another phenomenon that may be produced by the HAARP IRI, but apparently was not part of the summer campaign, involves RF mixing in the ionosphere. When HAARP HF transmissions are modulated (FM or AM) at approximately 3 Hz to 30 kHz rates and heat the ionosphere, RF mixing or demodulation can take place there that produces ELF through VLF radio waves (figure 3). The low frequency emissions can propagate over great distances in the Earth-ionosphere waveguide. I was not aware of this effect until after the summer experiment was completed so I did not attempt to detect it.

Although I expect the low frequency emissions to be weak (I estimate the received field strength to be on the order of a couple hundred µV m^{-1}), I may attempt to receive them during a future campaign using the VLF/LF loop antenna and receiver I installed at CRO during June 2018 (see {ReeveVLF}). Of course, the distance between HAARP and Cohoe is not a "great distance" (it is about 400 km), but attempting to receive these low frequency emissions would be yet another interesting aspect of HAARP operation.
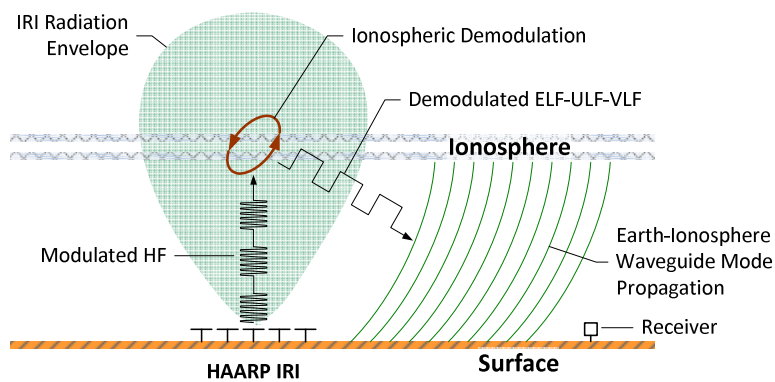
Figure 3 ~ Low frequency radio waves may be produced by ionospheric demodulation of the modulated signals from the HAARP IRI. These emissions then propagate over great distances in the Earth-ionosphere waveguide. Image adapted from {DTIC}

3. Receiver and Antenna Systems

The locations and other attributes of the transmitting and receiving stations are given in table 1. The major equipment items used at Cohoe Radio Observatory for these observations consist of the LWA antenna system, two different software defined radio (SDR) receivers, an RFSpace Cloud-IQ and SDRPlay RSP2Pro, and an Icom R-75 general coverage receiver (figure 4). The respective software is SpectraVue and SDRuno for the SDR receivers

and Radio-SkyPipe for the analog R-75. Because I was busy tuning and monitoring the two SDR receivers, I did not obtain any usable data with the R-75 receiver and Radio-SkyPipe. The CRO also has a dual Callisto installation but its present frequency range only extends down to 45 MHz, which is not low enough to receive HAARP transmissions – the maximum IRI frequency is 10 MHz.

Table 1 ~ Transmitting and receiving station characteristics
(AMSL: above mean sea level; AGL: above ground level, TN: True North)

Station	Function	Latitude	Longitude	Elevation (m AMSL)	Antenna height (m AGL)	Distance (km)	Direction (°TN)
HAARP (IRI)	Transmit	62° 23' 32.7" N	145° 09' 02.0" W	570	22	398	53 ↔ 238
Cohoe	Receive	60° 22' 04.8"N	151° 18' 54.5"W	22	1		
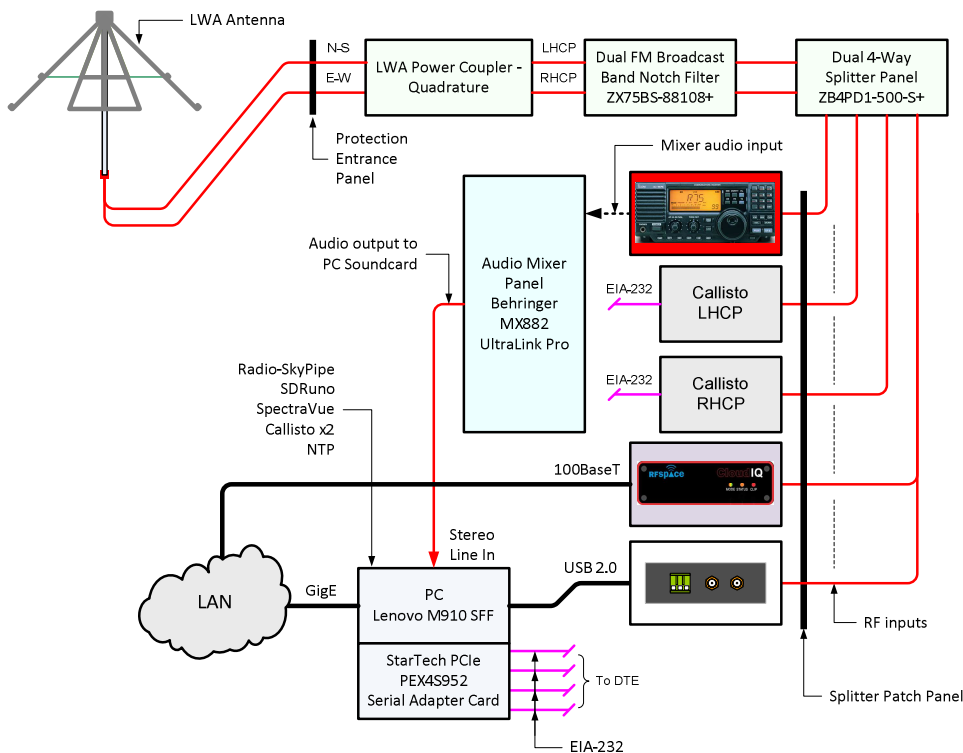
Figure 4 ~ System block diagram at Cohoe Radio Observatory. The LWA antenna provides two independent cross-polarized connections to a quadrature coupler. The R-75 shown at the top of the receiver stack is a general coverage receiver that is connected to the PC soundcard through an audio mixer. The RSP2Pro SDR receiver at the bottom of the stack connects to the PC via a USB 2.0 connection. The Cloud-IQ immediately above it uses a 100BaseT Ethernet connection. The Callistos as shown do not cover the necessary frequency range. Image © 2018 W. Reeve

The HAARP transmissions can propagate via ground wave, sky wave and near-vertical incidence skywave (NVIS); I suspect that NVIS is involved in most situations observed here. The great circle azimuth to the HAARP site from Cohoe and the elevation angle at Cohoe for observations of the ionosphere directly above HAARP (figure 5) are calculated from {Reeve14-1} and {Reeve14-2}. The great circle path between the two sites is for practical purposes entirely over land (figure 6).

The LWA antenna (figure 7) is a sloping crossed-dipole assembly and, at CRO, it is connected through an LWA Power Coupler with quadrature coupler to two identical RF splitters for distribution to the receivers. Its normal operating frequency range is approximately 5 to 90 MHz but it is usable at lower frequencies as is demonstrated later. The antenna's front-end electronics (FEE) are designed for 500 kHz to 115 MHz. The antenna is omni-directional with a squashed hemispherical vertical pattern (figure 8).

The local RF transmission chain includes the LWA antenna and associated cables and splitters (figure 9). The FEE gain is 35 dB. The losses in the two splitter stages are about 13 dB. The coaxial interconnection cables and quadrature coupler introduce another 5 dB. To prevent receiver overload I experimented with external attenuators on the receiver inputs and ended up using 10 or 20 dB depending on the receiver. This is discussed more below.
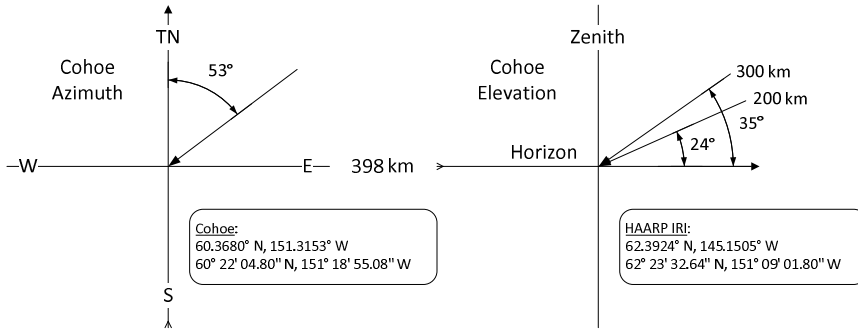
Figure 5 ~ Azimuth (left) and elevation (right) for propagation path to the F-region ionosphere directly above the HAARP site; these assume a vertical beam at HAARP. Different beam angles will change the values slightly. Two ionosphere heights are shown because it can vary. Azimuth is with respect to True North (TN). Image © 2018 W. Reeve

Figure 6 ~ Great circle propagation path between the airports nearest to the Cohoe and HAARP sites, Kasilof (5KS) and Gulkana (GKN), respectively. The path is mostly over mountainous terrain. Underlying image produced by Great Circle Mapper {GCMap}

Figure 7 ~ Long Wavelength Array (LWA) antenna at Cohoe Radio Observatory. The crossed-dipole assembly is protected from rampaging moose by the wood fence and is placed with a ground screen on a sandy-gravel pad behind the observatory building. The pad is shown entirely in this image, and its dimensions are 7.6 x 7.6 m. The antenna itself is 1.5 m high. Image © 2018 W. Reeve
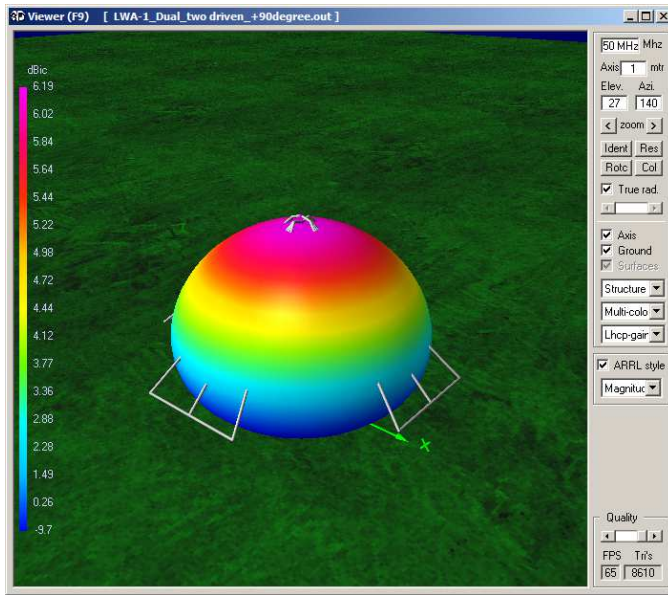
Figure 8 ~ Long Wavelength Array antenna radiation pattern. The antenna is most sensitive near vertical but has good response at low angles as well. The 3-D image shown here was produced by 4NEC2 numerical electromagnetic code modeling software {4NEC2}. A description of the LWA antenna model may be found at {ReeveLWA}.
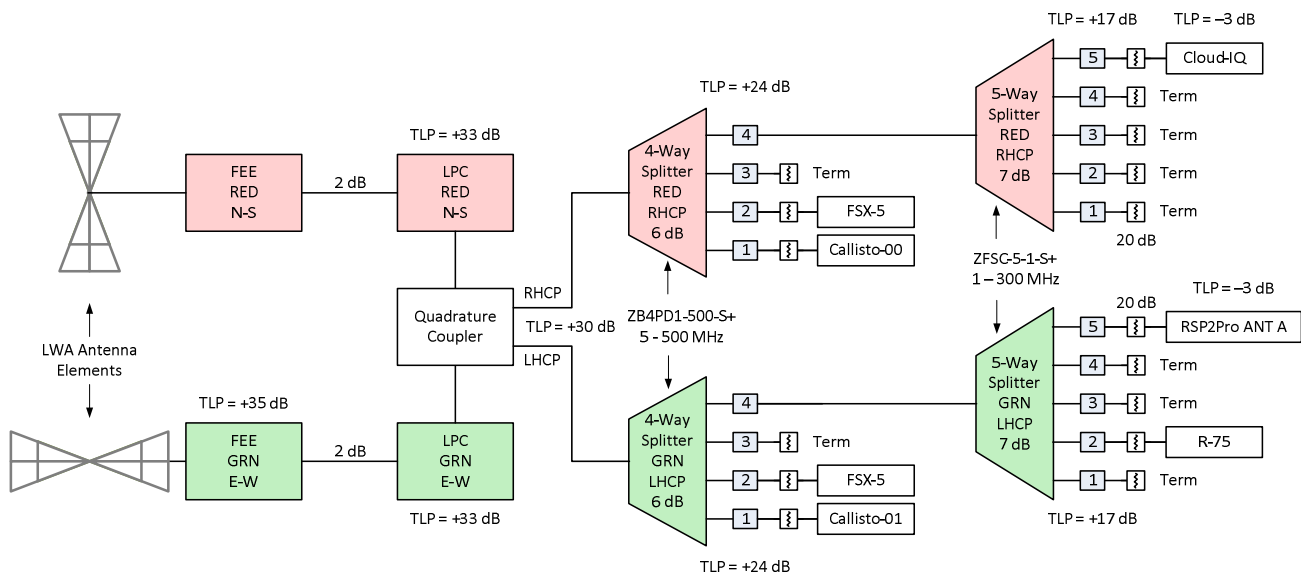
Figure 9 ~ RF transmission level diagram for the LWA antenna and receiver systems at CRO. All transmission levels shown are nominal. All unused splitter ports are terminated in 50 ohms. TLP: Transmission Level Point. Image © 2018 W. Reeve

The splitter outputs are right-hand and left-hand circularly polarized signals. I connected the SDR receivers to different splitters (different polarizations). In retrospect I should have connected the receivers to the same splitter so I could directly compare the spectrums. HAARP transmitted both ordinary (O) and extraordinary (X) mode circular polarized signals at various times, but because of my inattention I did not properly exploit the polarization capabilities of the LWA antenna system. This will be another aspect of HAARP operation that I will investigate in the future.

I found early on that the Cloud-IQ with SpectraVue provided much better results than the RSP2Pro with SDRuno. Many of the received signals from HAARP were quite strong and I was not able to find a gain setting on the RSP2Pro receiver that provided a good spectrum display (shown in the next section). I tried different external

input attenuators and all possible software gain settings but never could achieve comparable results. There may have been strong out-of-band interference causing problems with the RSP2Pro, but the SDRuno software never indicated an overload condition. At the next opportunity I plan to try different combinations of lowpass, bandpass and highpass filters to eliminate the possibility of front-end overload from out-of-band signals. I experienced no similar problems with the Cloud-IQ receiver – it never indicated any problems even with the internal attenuator set to 0 dB, and SpectraVue always provided a good display.

I simultaneously recorded Waveform Audio File Format (.wav) files for later analysis using both SpectraVue and SDRuno (despite its name, a WAV file is not limited to audio). Because the Cloud-IQ receiver does some upstream signal processing (preprocessing), the data stream from it is somewhat lower than the RSP2Pro. The preprocessing and ability to record several specific time intervals resulted in a considerably smaller amount of data compared to SDRuno.

Over the campaign's three days I recorded 125 WAV files with SpectraVue, which required a total of 73 GB of storage. Each WAV file was about 684 MB with durations between 3 and 15 min. Although a given recording session typically consisted of several separate files, the files are played back seamlessly and in sequence by SpectraVue. A series of schedules can be prepared in SpectraVue beforehand, so I usually scheduled two or three sequential recordings based on information provided by HAARP Chief Scientist, Dr. Chris Fallen. While one schedule was running, I could make minor adjustments to the following schedules to accommodate last-minute changes, if needed. On the other hand, SDRuno allows only one recording to be scheduled at a time, so I set it to run the whole of each of two afternoons. This resulted in quite a bit of useless data because the recorder was running even though no experiment was in progress, but it relieved me of having to keep track of two separate recorders.

I only recorded two days with SDRuno, which resulted in 133 files with a total storage requirement of 257 GB. SDRuno does not include the receiver gain setting in the WAV file metadata so the displayed power levels on playback are incorrect. However, if the gain is known for that recording session it can be manually entered prior to the WAV file playback and the displayed power level will then be correct. There is another inconvenience with SDRuno: A receiver must be attached to the PC for the software to run and to playback the WAV file, and for correct gain the receiver must be the same type as used in the original recording.

---

4. Observations

The experiments started around local noon and ended in the late afternoon between around 2000 and 0100 UTC on each of the experiment days 30 and 31 July and 1 August. I noted occasional differences between Dr. Fallen's tweeted frequencies and times and what I actually received. However, I expected some differences because the frequencies and times may be changed at the last minute to accommodate real-time ionospheric characteristics or the last minute changes of the individual investigators. Transmitted carrier frequencies varied from as low as 2.7 MHz to as high as 9.5 MHz, encompassing almost the full range of the IRI.

The WSPR transmissions took place at different times than the other experiments, usually at the end of each experiment day. These transmissions were in the 80 m (3.5686 MHz, although 3.5926 MHz was incorrectly used in some early sessions) and 40 m (7.0386 MHz) radio amateur bands. Although I made no attempt to use the

WSPR reporting function, I did detect the transmissions. Reduced IRI array configurations were used during the WSPR portions of the campaign. These included 2x2 and 8x8 antenna configurations and various beam directions and power levels. Beam directions were along magnetic field lines and vertical. Generally, the WSPR transmissions received at Cohoe were weak but there were occasional enhancements. The stronger signals probably were received by near-vertical incidence skywave (NVIS) from the larger array configurations and higher transmitted power levels as well as preferential directions into the ionosphere with respect to magnetic field lines and electron density profiles.

I used both wideband and narrowband receiver setups throughout the campaign but did not record all transmissions. When I did not have firm details on frequencies, I setup the SDR receiver software to display a wide frequency span from 2.5 to 10.5 MHz (the full IRI frequency range). At other times I set the software to display a narrower span of 100 kHz or less depending on how much detail I wanted to view in the received spectrum. In a few sessions I setup the software on the wrong center frequency and missed the frequencies actually being used. Some of the SpectraVue spectrums are averaged, usually no more than 5 FFT averages as indicated in the control area of the window on the left side below the waterfall. Averaging also was used on the SDRuno spectrums but it is not indicated and I did not log the setting.

The first two days involved multi-carrier transmissions with various numbers of channels and various frequency offsets. The multi-carrier transmissions had up to six frequencies but sometimes I did not receive all the carriers because some were too weak or not actually transmitted. Generally, the offset between frequencies was a fixed value for each transmission set. For example, six channels with 8 kHz separation (offset) would be transmitted for 2.5 min, the IRI turned off for 0.5 min, and then six channels with 10 kHz separation would be transmitted for 2.5 min, and so on.

I occasionally snapped screenshots of interesting activity during the live sessions. Also, a few days after the campaign finished I played back all WAV files and made a log of the activities (see **Appendix**) and then captured screenshots of a few of the more interesting spectrums displays (figure 10). These screenshots make up the rest of this section; additional screenshots are shown in the next section. In SpectraVue, the time of a live screenshot appears in the lower-right of the window while in a playback screenshot the time appears in the lower-middle. SDRuno provides no timestamps unless they are enabled in the Main Spectrum (SP1) window setup. In some SpectraVue screenshots demodulation was enabled and is seen as a shaded area on the spectrum. The demodulation does not affect the display, only the audio heard during live or recording playback.
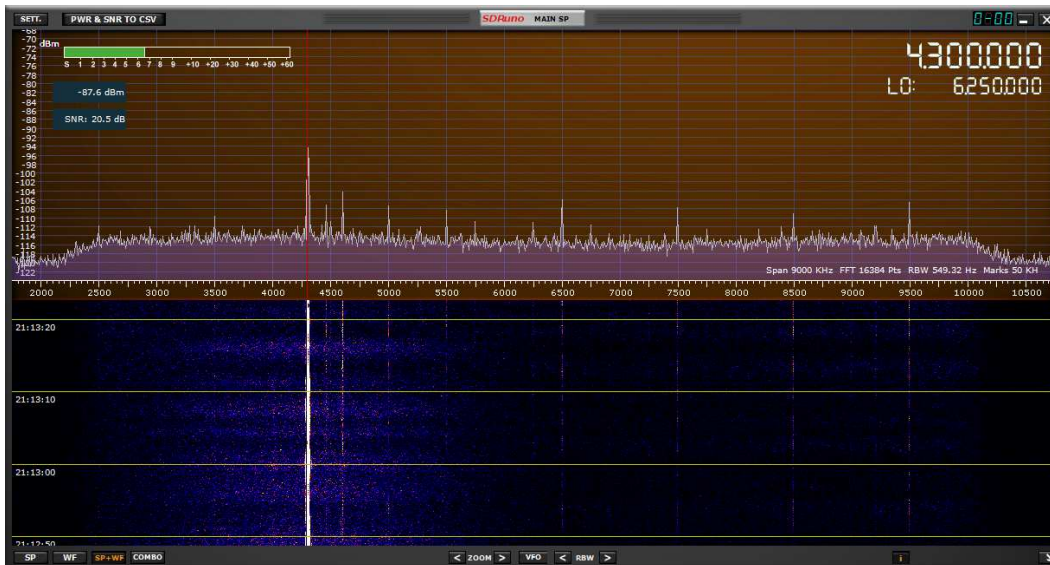
Figure 10.a ~ Comparison of SDRuno and SpectraVue spectrum/waterfall displays for multi-carrier reception on 30 July 2018, 2113 UTC, 4.3 MHz. Both displays have 8 MHz span.

The individual carriers are not visible because of the wide frequency spans. Note the differences in the displayed noise and power levels in the two spectrums. Both receivers have a 20 dB attenuator on their RF inputs. Both images were made during live reception.
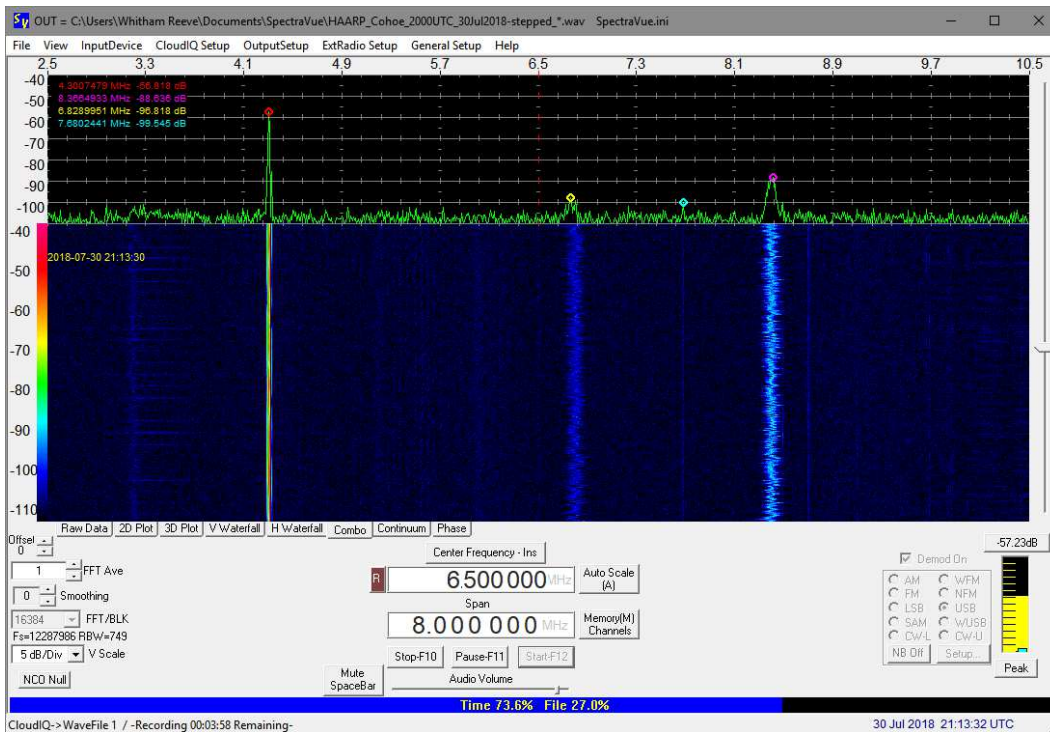
Top: SDRuno center frequency is 6.25 MHz and the 4.3 MHz carriers are seen at the position of the red cursor.

Bottom: SpectraVue center frequency is 6.5 MHz and the 4.3 MHz carriers are seen as a strong single carrier in the left portion of the image.
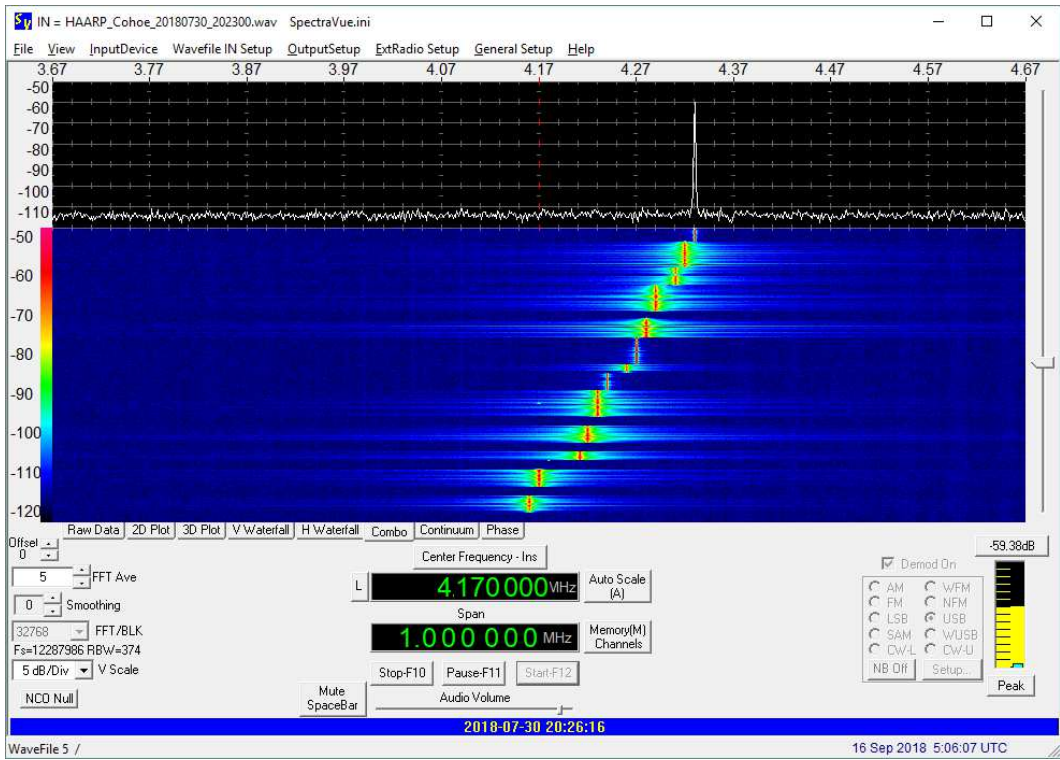
Figure 10.b ~ Stepped carrier, 30 July 2018, 2026 UTC. Playback: Display centered at 4.17 MHz. the step size and transmission time duration varies. The "blooming" effect may be due to the modulation being used. It is not caused by the receiver or software – it disappears during reception of the last carrier displayed here.
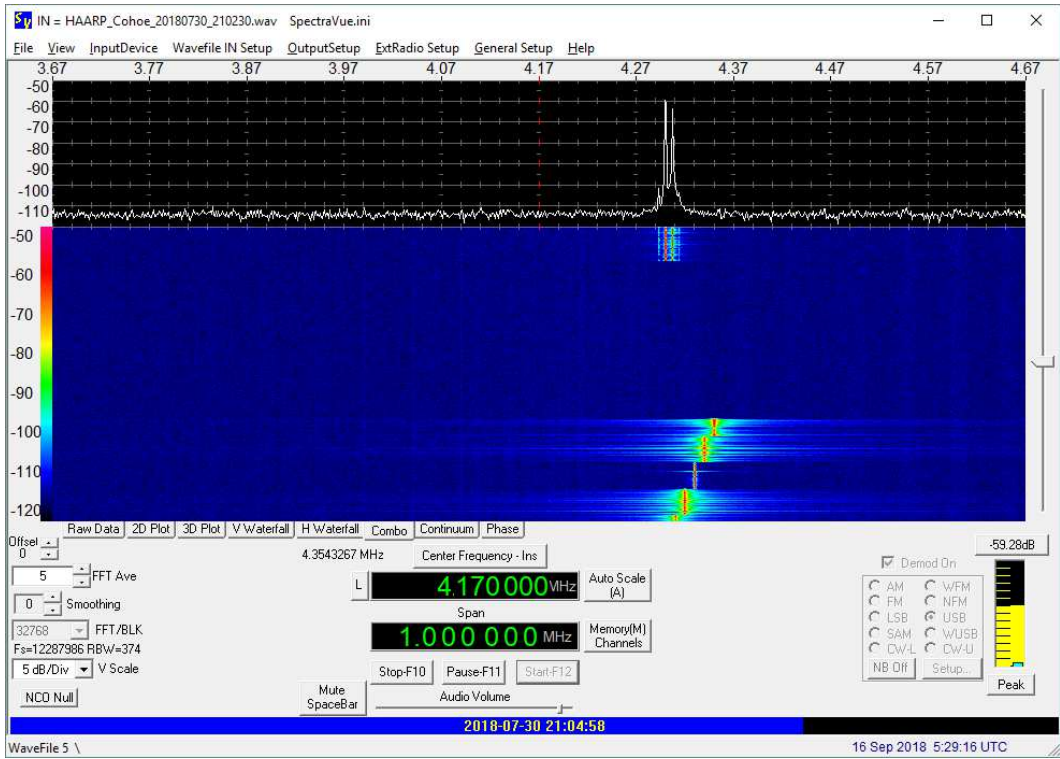
Figure 10.c ~ 30 July 2018, 2105 UTC. Playback: Stepped followed by multi-carrier, 4.17 MHz. There are a few minutes dead-time between the end of the stepped and multi-carrier transmissions.
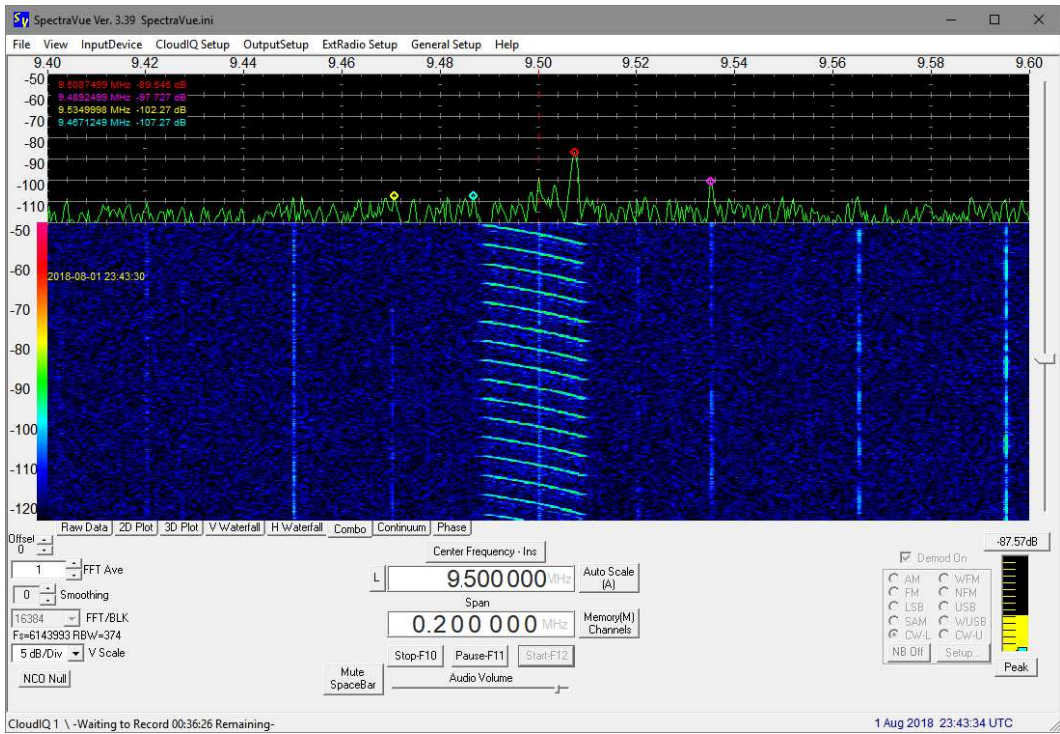
Figure 10.d ~ 01 August 2018, 2343 UTC. Live: 9.5 MHz, 200 kHz span, Frequency Modulation.
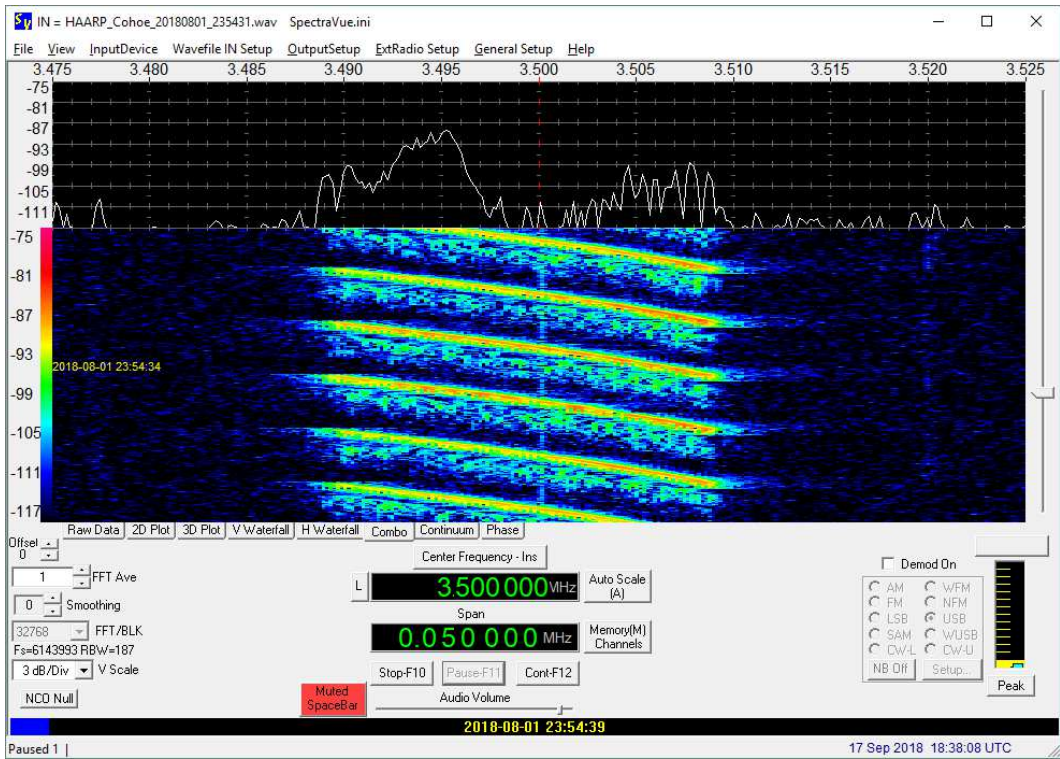
Figure 10.e ~ 01 August 2018, 2354 UTC. Playback: 9.5 MHz, 50 kHz span, Frequency Modulation.
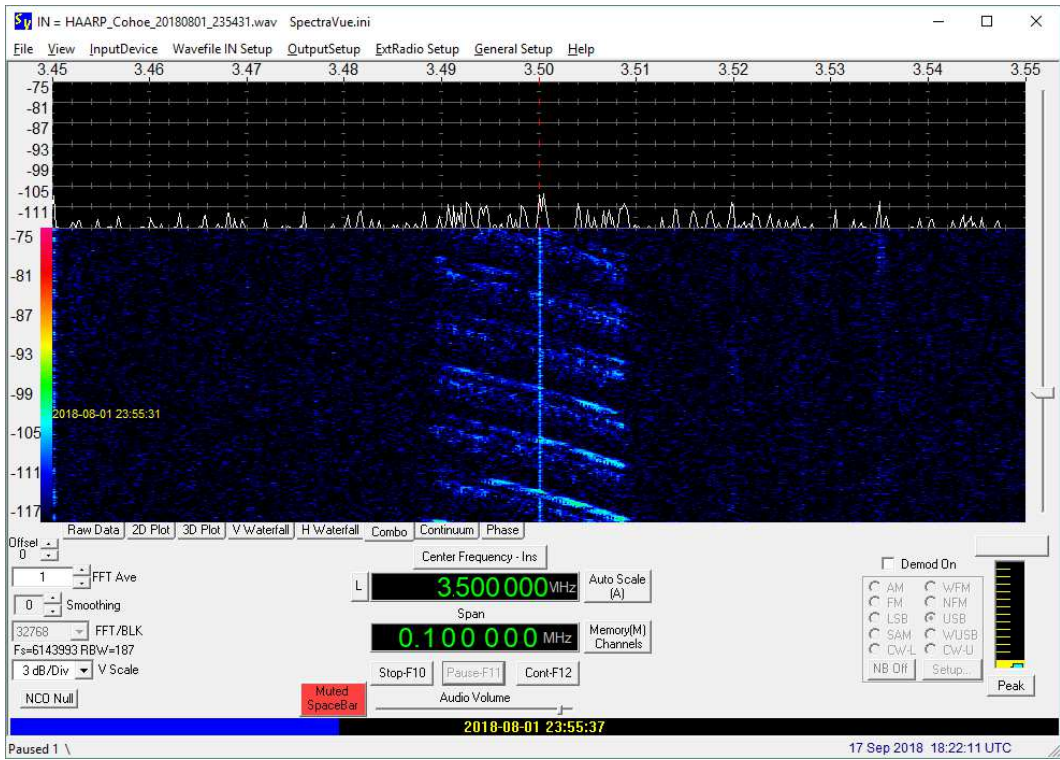
Figure 10.f ~ 01 August 2018, 2355 UTC. Playback: 9.5 MHz, 100 kHz span, Frequency Modulation, weak reception.
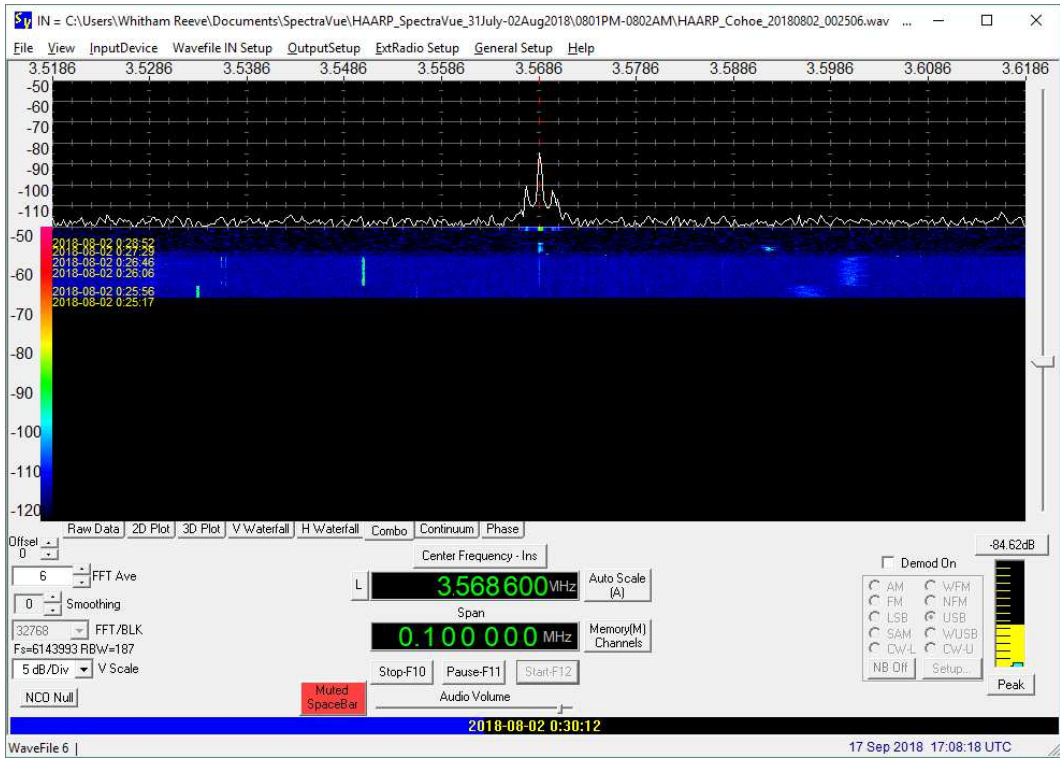
Figure 10.g ~ 02 August 2018, 0030 UTC. Playback: 3.5686 MHz (WSPR), 100 kHz span showing sidebands at approximately ±1500 Hz.

5. Additional Spectrum Screenshots

The spectrum images in this section were taken in real-time (live) and from recordings (playback), as indicated (figure 11, 12, 13, 14 and 15). The images are grouped by day and activity. There are some differences between

the time and frequency log in the **Appendix** and the actual event shown in the images. This is discussed briefly in the **Appendix**.

30 July 2018: The following four images show the problems I had using SDRuno software and the RSP2Pro receiver. The receiver input signal levels were identical to the levels input to the Cloud-IQ receiver. Note the spectral noise hump centered on the receiver frequency. I experimented with various gain settings and input attenuators but could never attain a display in SDRuno that was equivalent to SpectraVue.
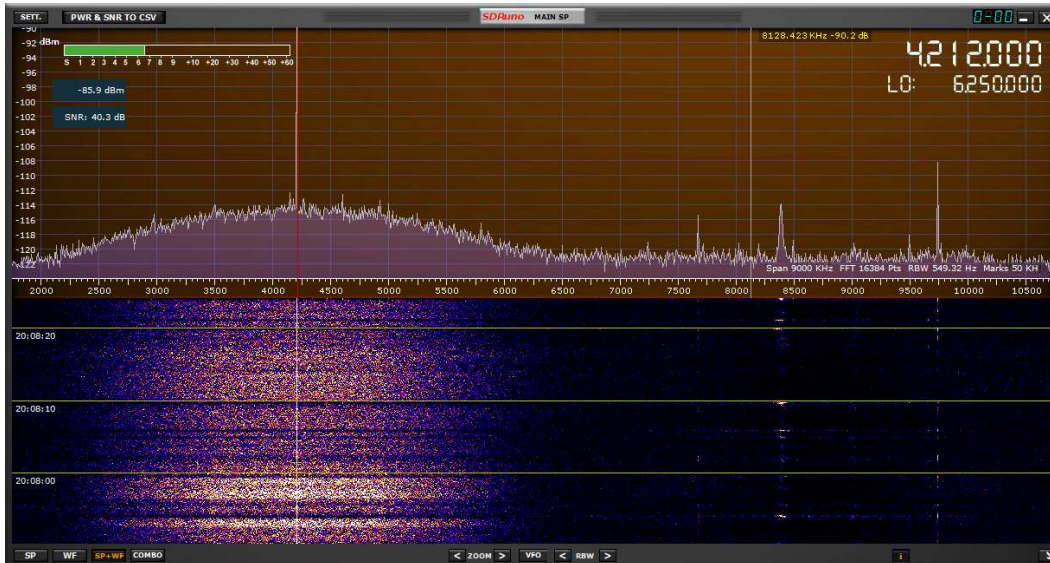
Figure 11.a ~ SDRuno: 2008 UTC, 30 July, Live: 4.212 MHz. Displayed frequency span is 8 MHz.
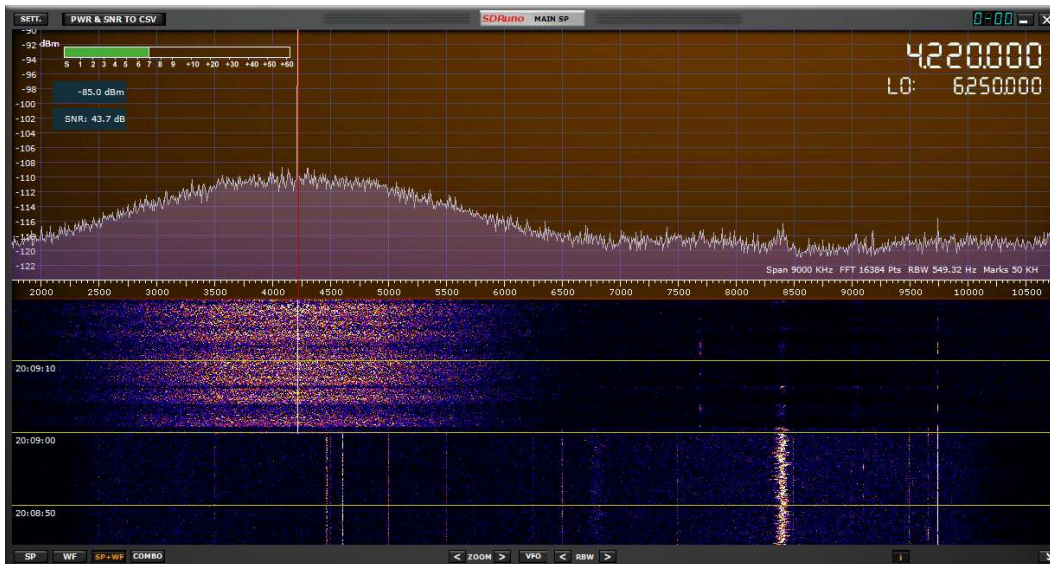
Figure 11.b ~ SDRuno: 2009 UTC, 30 July, Live: 4.220 MHz. Displayed frequency span is 8 MHz.
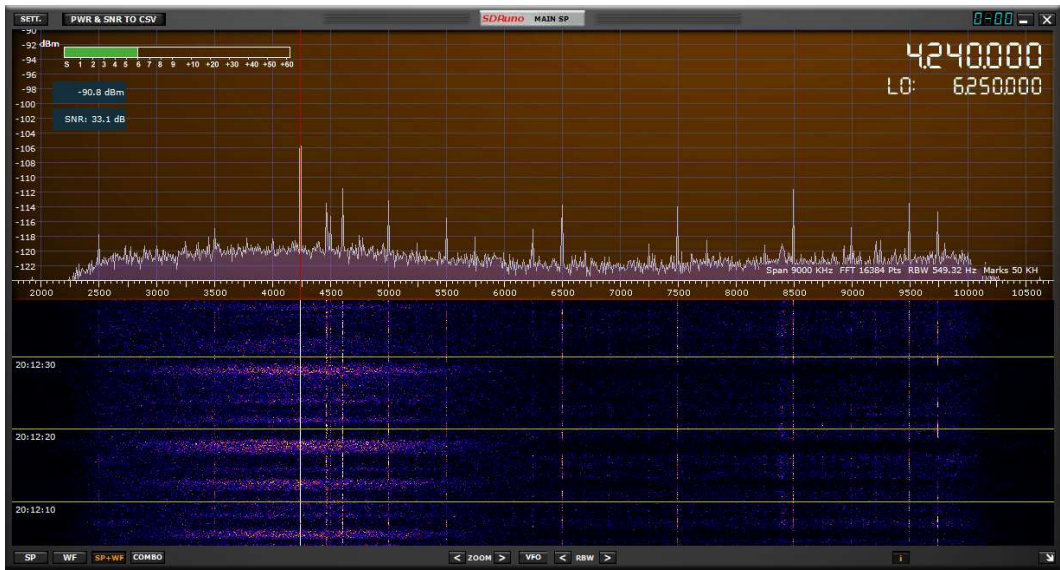
Figure 11.c ~ SDRuno: 2012 UTC, 30 July, Live: 4.240 MHz. 30 dB attenuator. Displayed frequency span is 8 MHz.
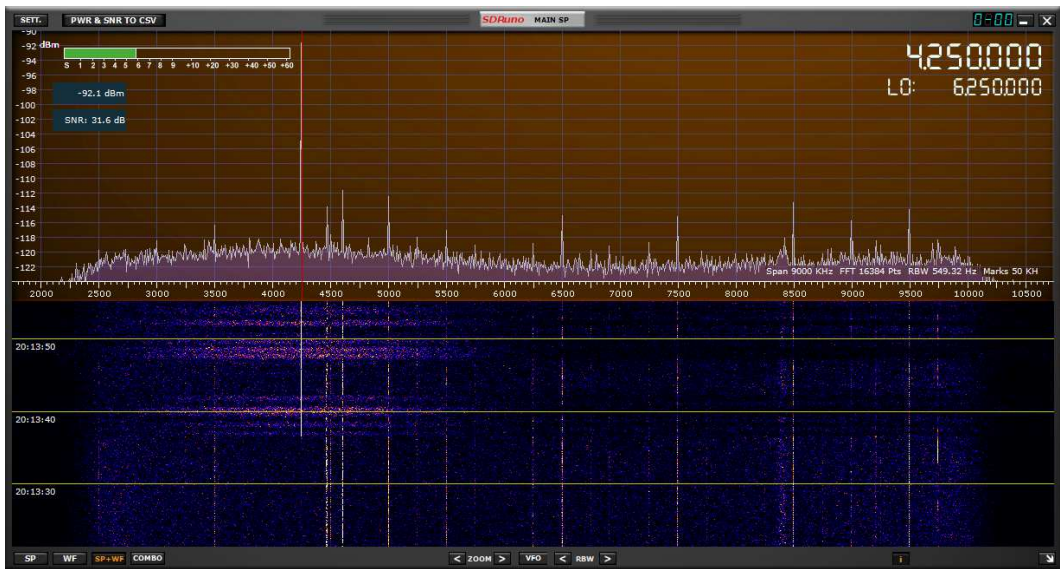
Figure 11.d ~ SDRuno: 2013 UTC, 30 July, Live: 4.250 MHz. 30 dB attenuator. Displayed frequency span is 8 MHz.
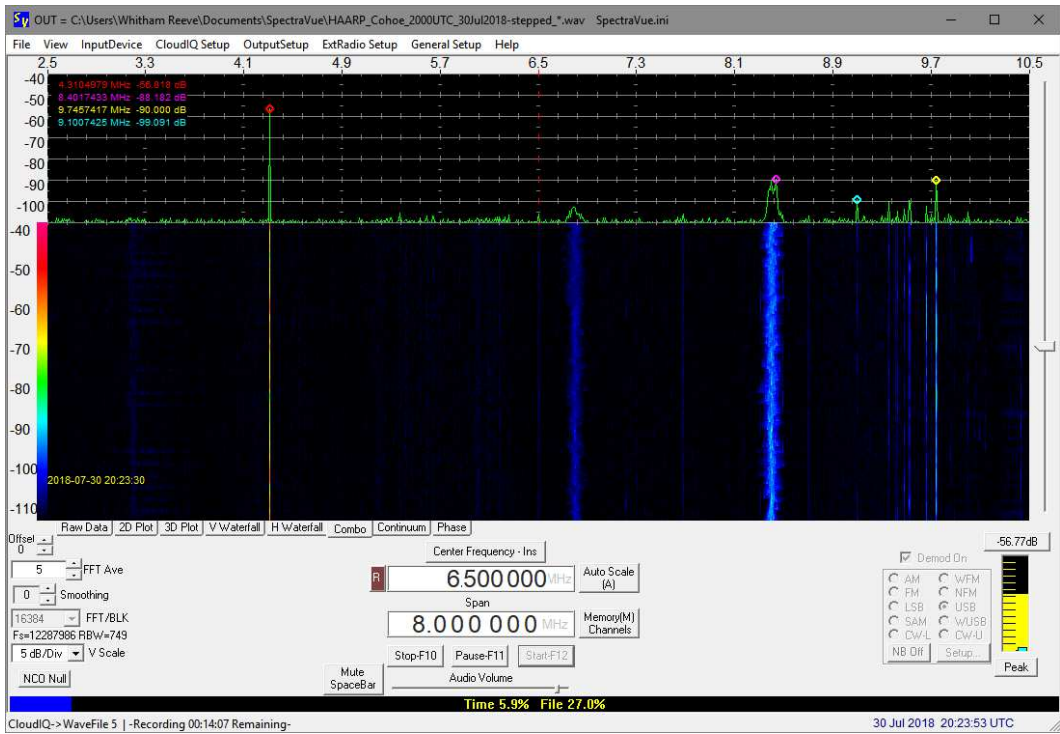
Figure 11.e ~ SpectraVue: 2023 UTC, 30 July, Live: 4.310 MHz. Displayed frequency span is 8 MHz.
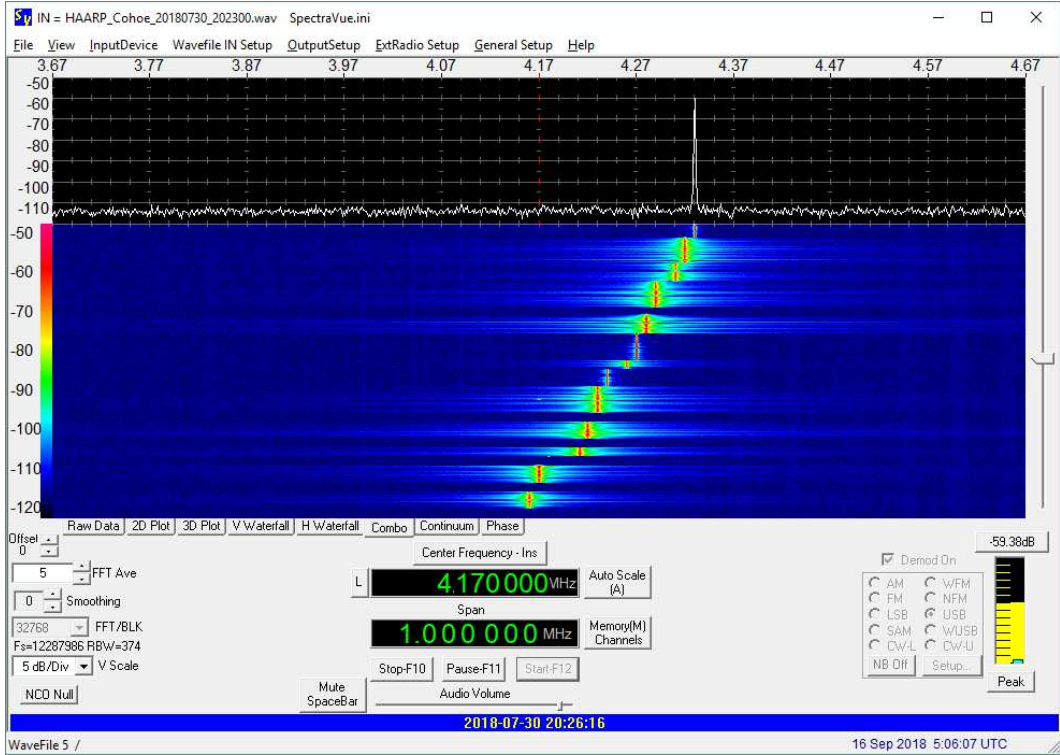
Figure 11.f ~ SpectraVue: 2026 UTC, 30 July, Recording: Stepped frequencies with different separation and duration. Displayed frequency span is 1 MHz.
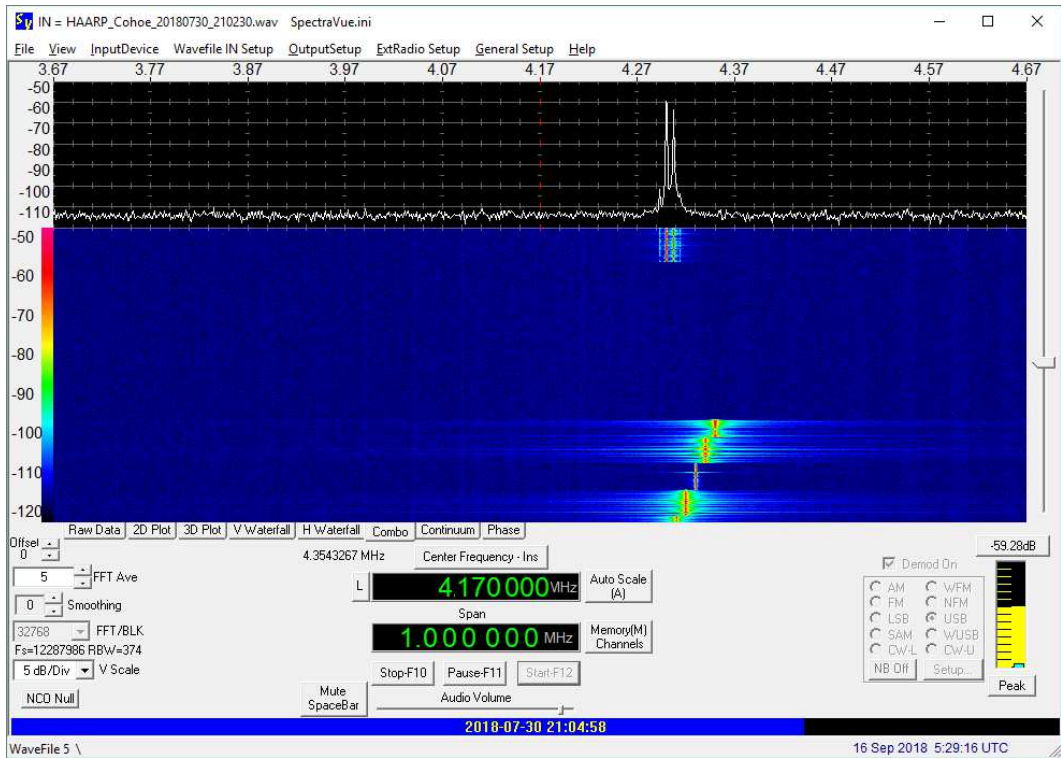
Figure 11.g ~ SpectraVue: 2104:58 UTC, 30 July, Playback: Stepped and multi-carrier: 4.293, 4.300, 4.307, 4.314 MHz, Δ = 7 kHz (on 21:03:00, off 2105:30). Displayed frequency span is 1 MHz.
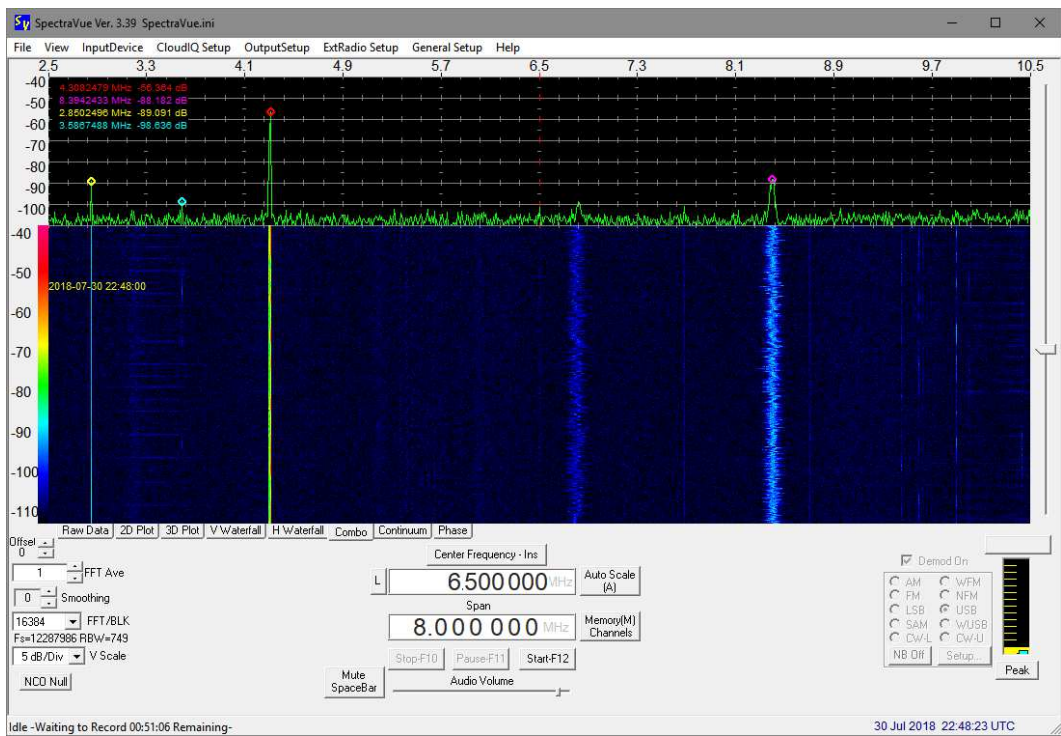
Figure 11.h ~ SpectraVue: 2248 UTC, 30 July, Live: 4.308 MHz. Displayed frequency span is 8 MHz.
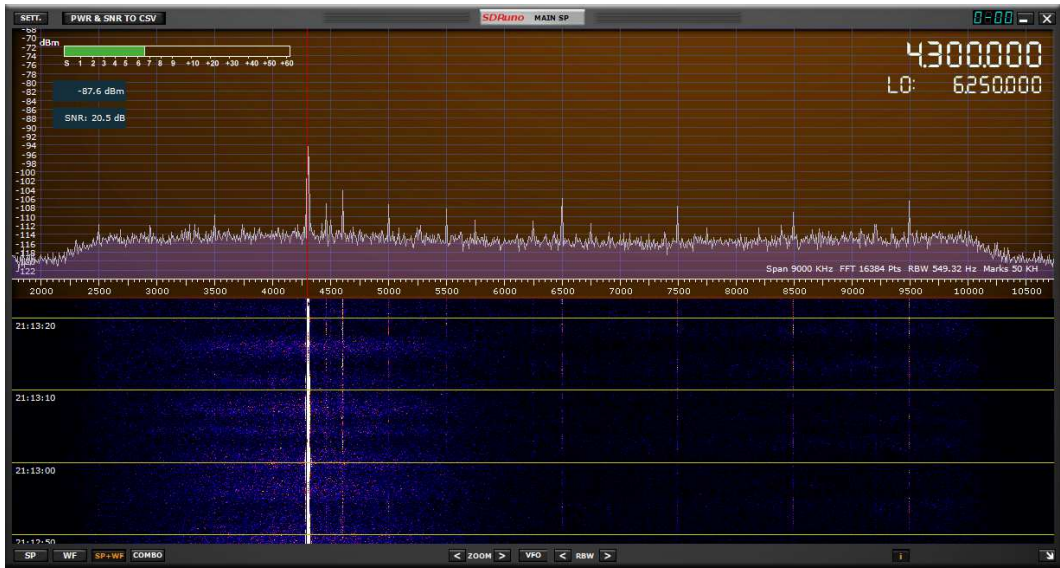
Figure 11.i ~ SDRuno: 2113 UTC, 30 July, Live: 4.288, 4.300, 4.312, 4.324 MHz, Δ = 12 kHz (on 2112:00, off 2114:30). Displayed frequency span is 8 MHz.
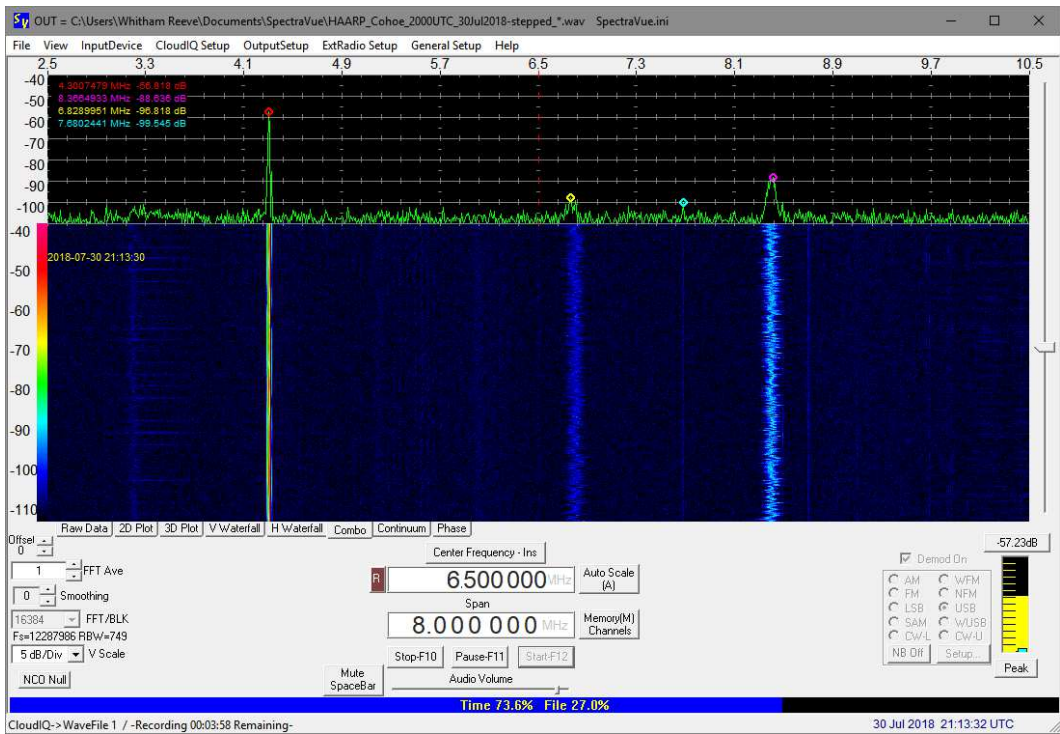
Figure 11.j ~ SpectraVue: 2113 UTC, 30 July, Live: 4.288, 4.300, 4.312, 4.324 MHz, Δ = 12 kHz (on 2112:00, off 2114:30). Displayed frequency span is 8 MHz.
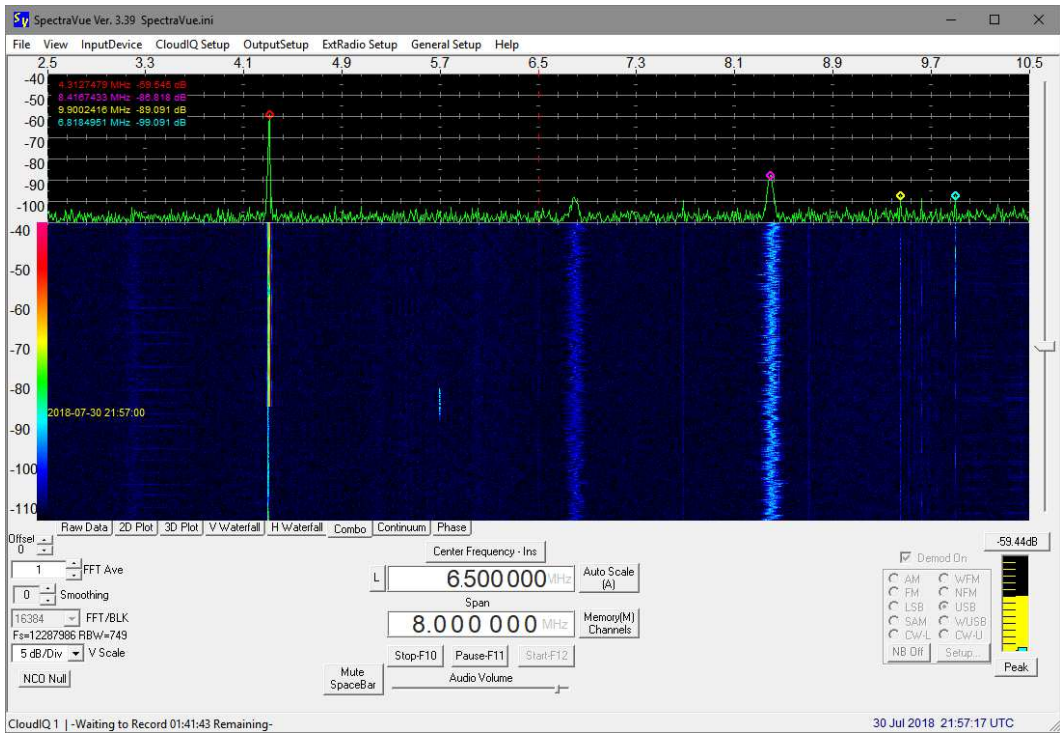
Figure 11.k ~ SpectraVue: 2157 UTC, 30 July, Live: 4.313 MHz. Displayed frequency span is 8 MHz.
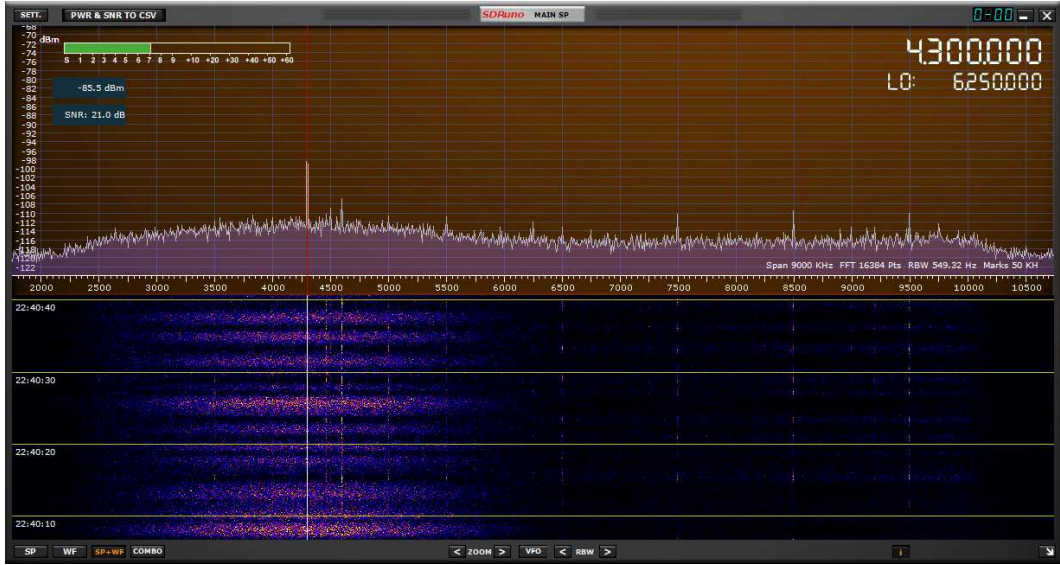
Figure 11.l ~ SDRuno: 2240 UTC, 30 July, Live: 4.300 MHz. Displayed frequency span is 8 MHz.

31 July 2018:
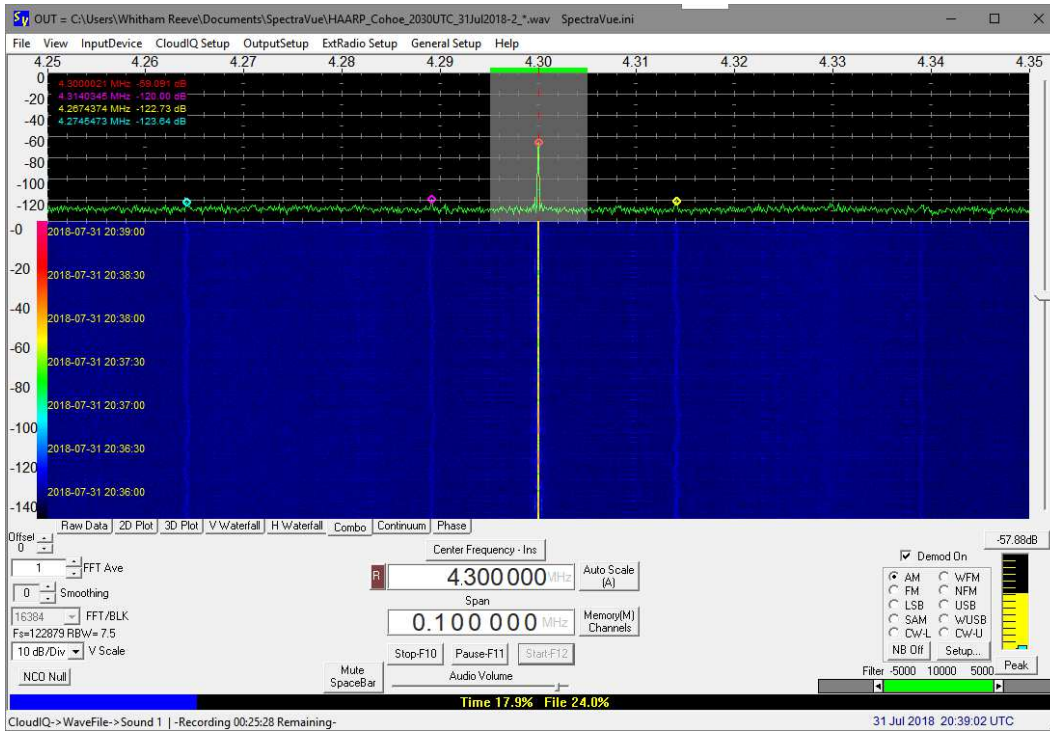
Figure 12.a ~ SpectraVue: 2039 UTC, 31 July, Live: 4.300 MHz. Displayed frequency span is 100 kHz and demodulation is set to AM.
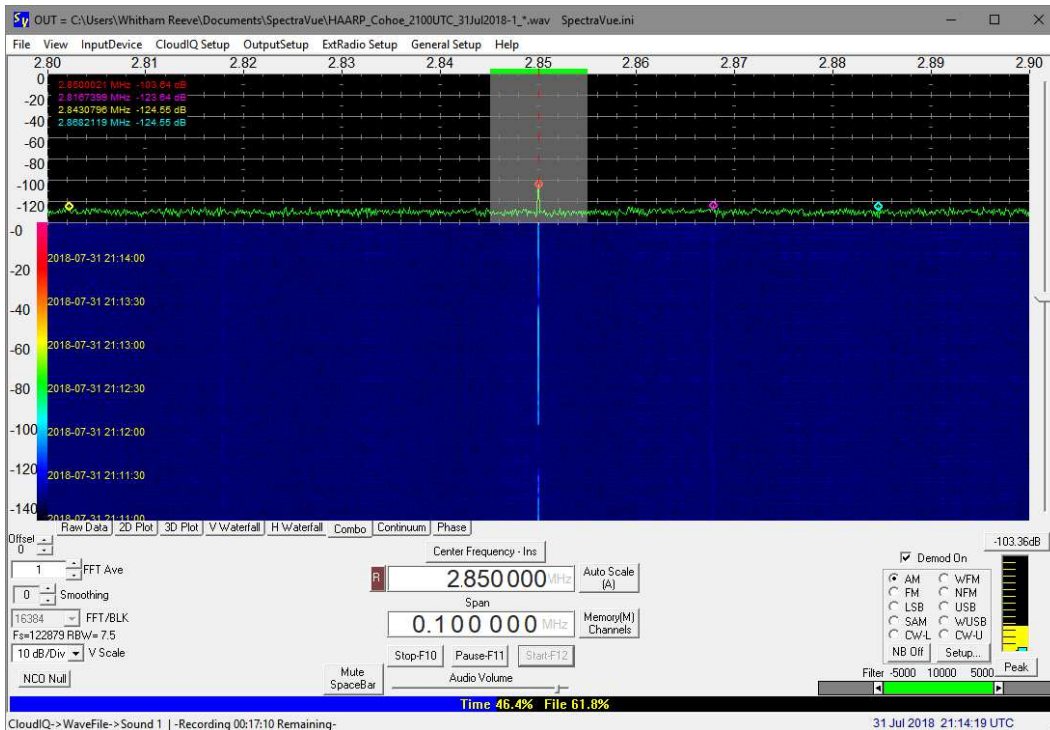
Figure 12.b ~ SpectraVue: 2114:19 UTC, 31 July, Live: 2.850 MHz. Displayed frequency span is 100 kHz and demodulation is set to AM.
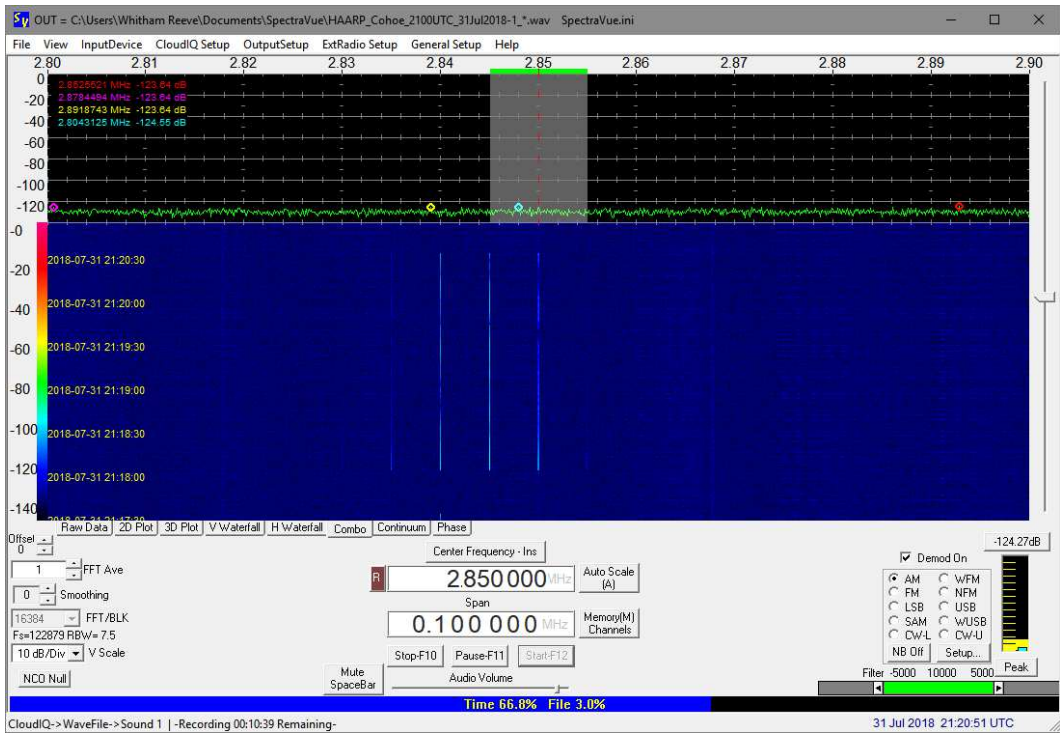
Figure 12.c ~ SpectraVue: 2120:51 UTC, 31 July, Live: Multi-carrier at 2.840, 2.846 and 2.852 MHz. Displayed frequency span is 100 kHz and demodulation is set to AM.
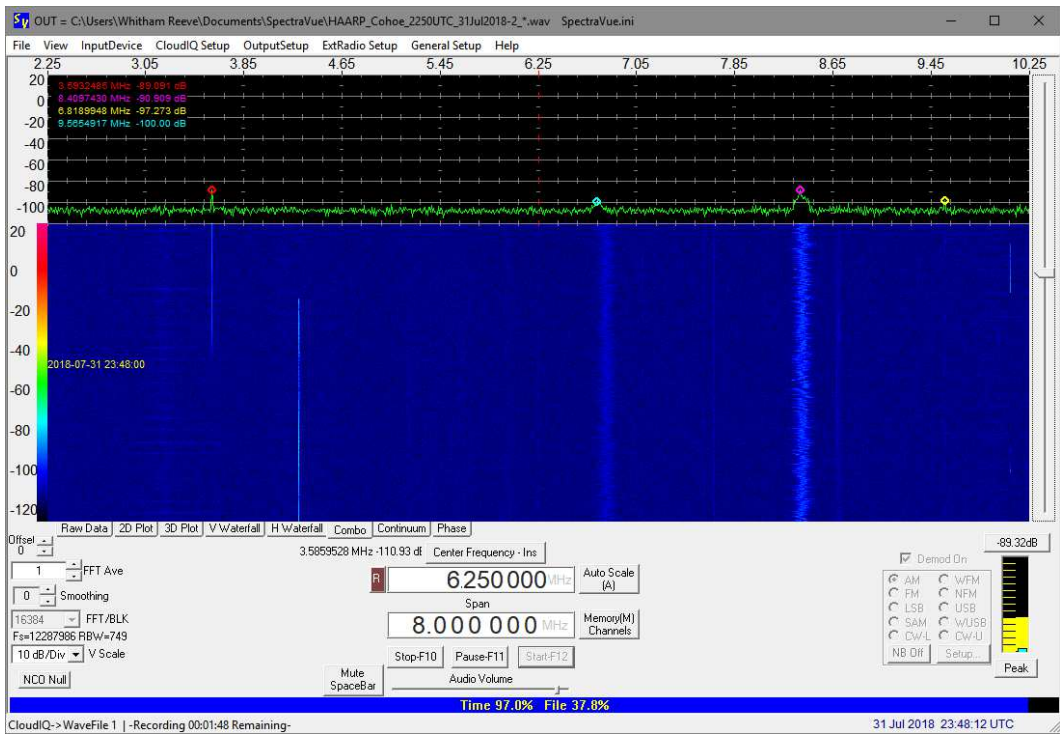
Figure 12.d ~ SpectraVue: 2348:12 UTC, 31 July, Live: 3.5926 WSPR. Displayed frequency span is 8 MHz with no demodulation.
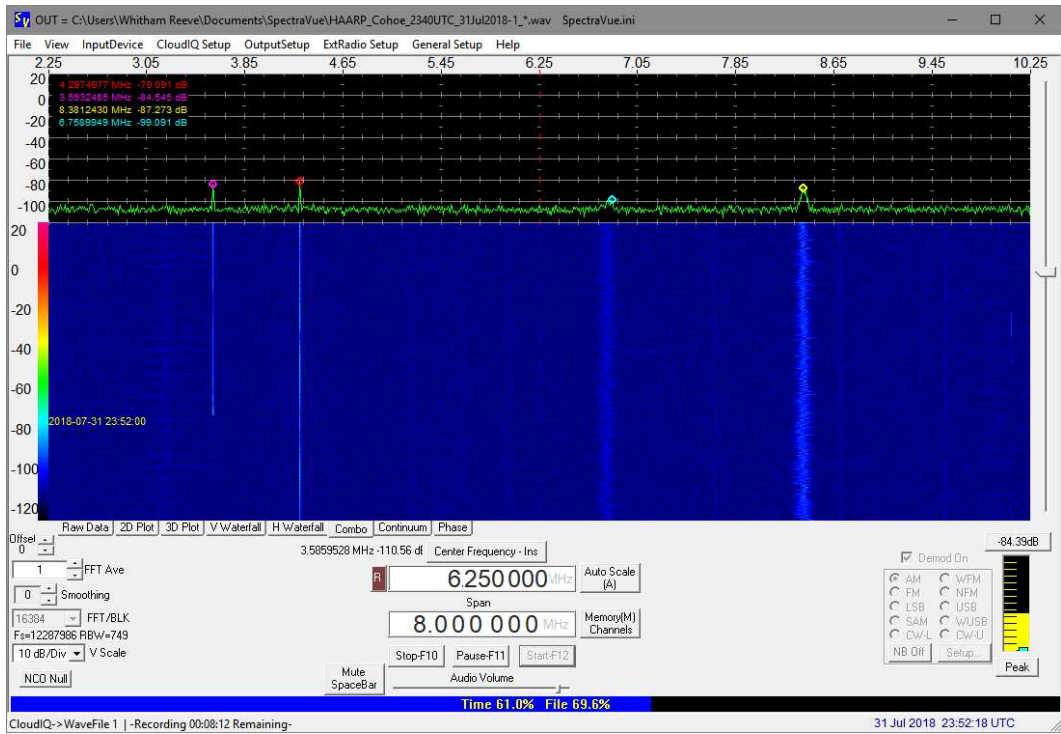
Figure 12.e ~ SpectraVue: 2352 UTC, 31 July, Live: 3.5926 MHz WSPR. Displayed frequency span is 8 MHz with no demodulation.
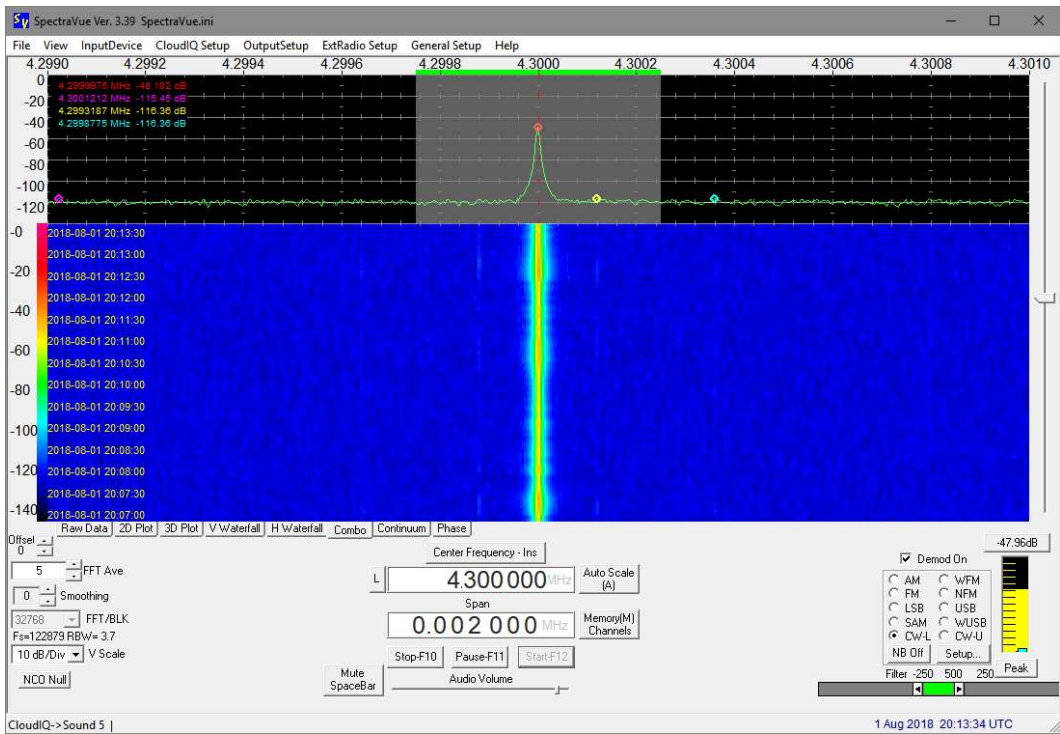
Figure 13.a ~ SpectraVue: 2013:34 UTC, 01 August, Live: 4.300 MHz, source of spectral blooming unknown but it may be due to the very high received signal levels. The displayed frequency span is 2000 Hz and demodulation is set to CW-low.
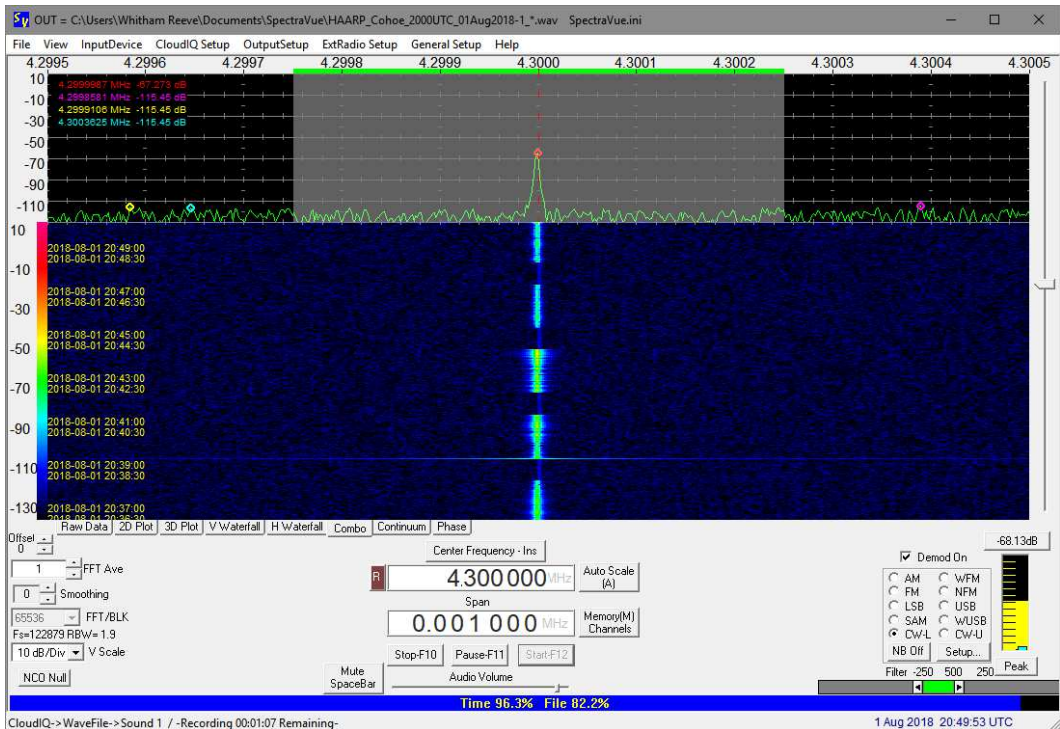
Figure 13.b ~ SpectraVue: 2049 UTC, 01 August, Live: 4.300 MHz. The shaded area in the spectrum indicates the limits of the filter used during demodulation, in this case CW-Low (sideband). The displayed frequency span is 1000 Hz and demodulation is set to CW-low.
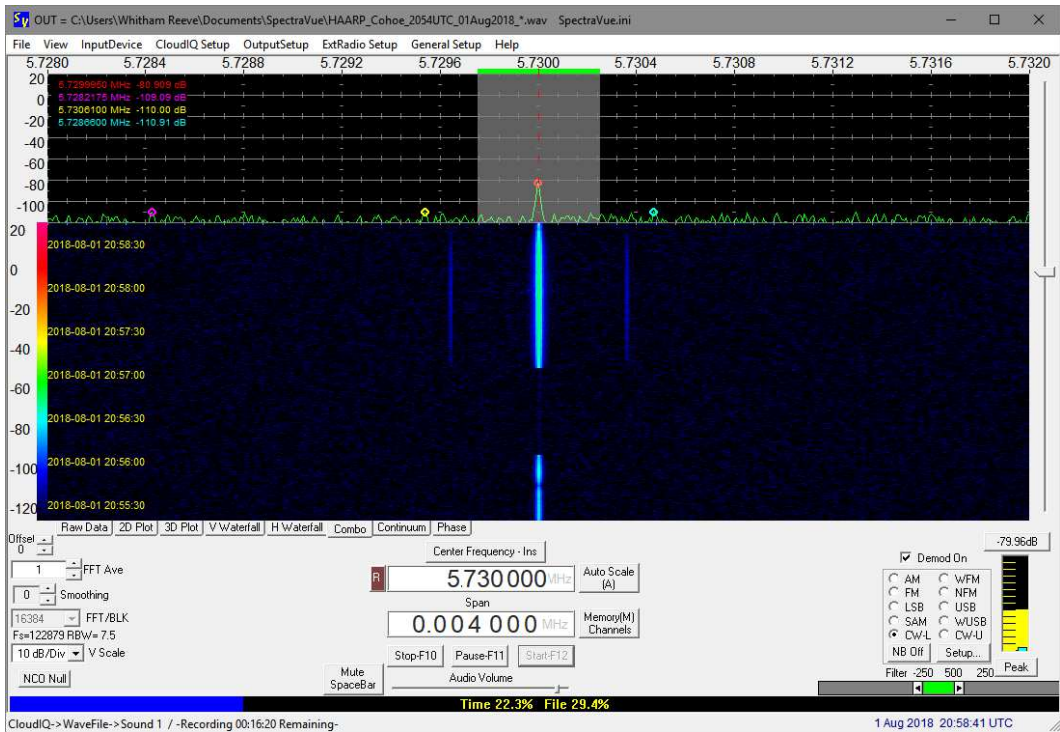
Figure 13.c ~ SpectraVue: 2058 UTC, 01 August, Live: 5.730 MHz. Displayed frequency span is 4000 Hz and demodulation is set to CW-low.
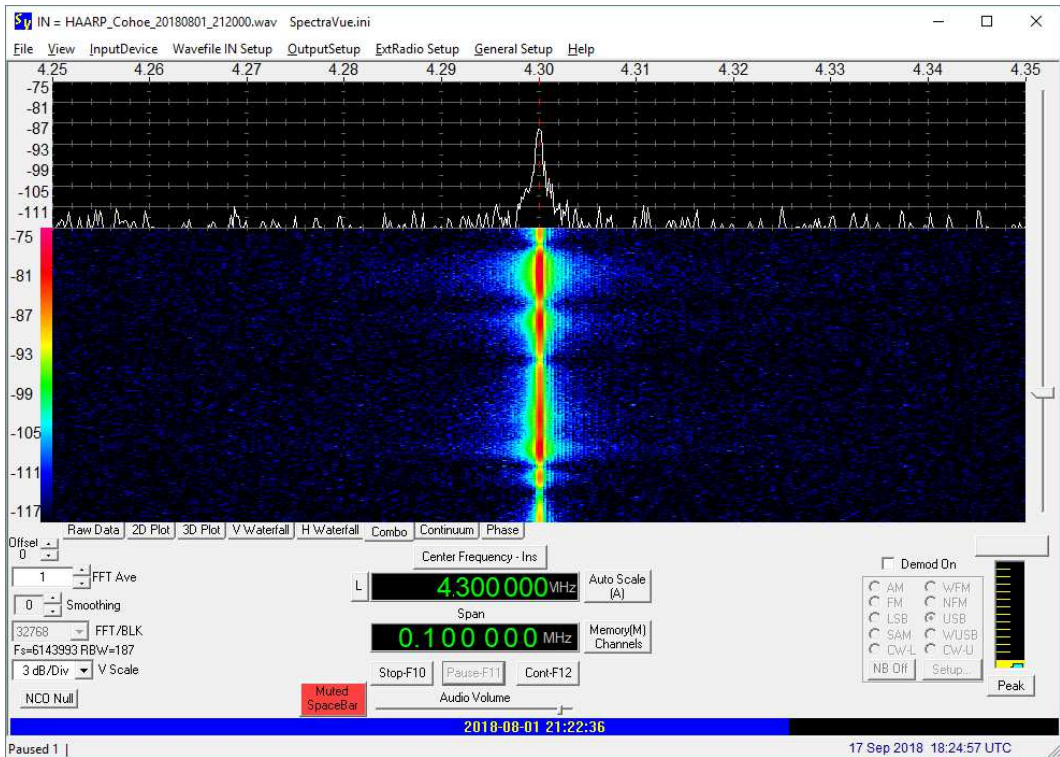
Figure 13.d ~ SpectraVue: 2122 UTC, 01 August, Recording: 4.300 MHz. No demodulation was used. Displayed frequency span is 100 kHz with no demodulation.
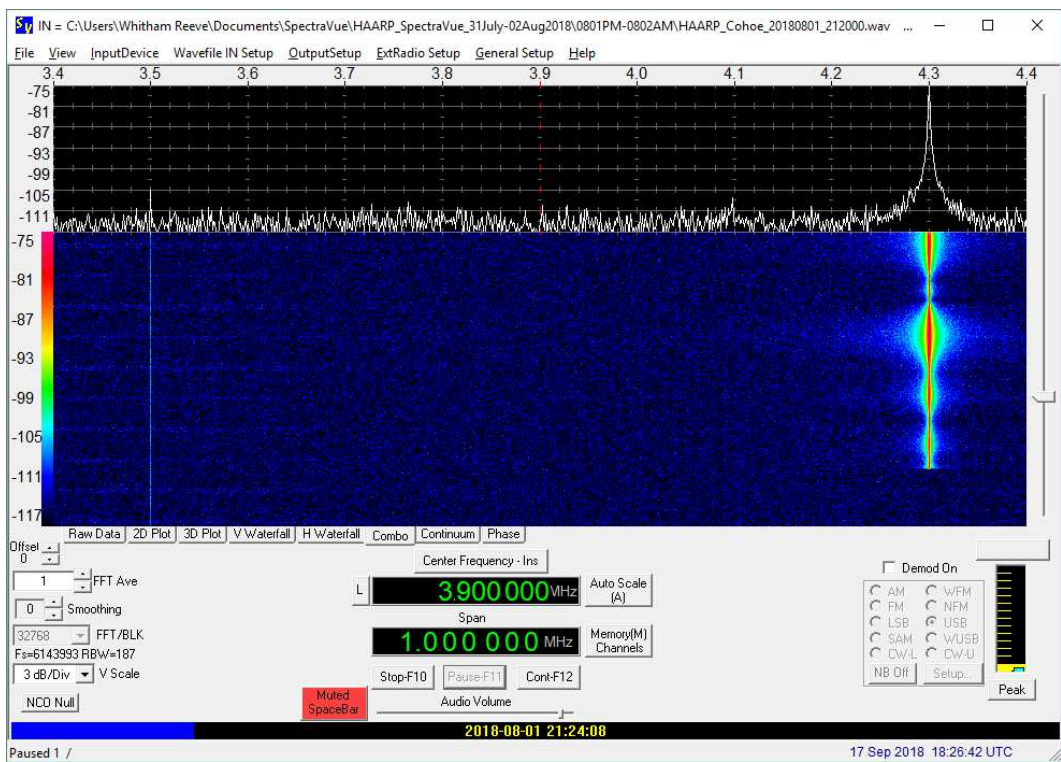
Figure 13.e ~ SpectraVue: 2124:08 UTC, 01 August, Recording: 4.300 MHz. Displayed frequency span is 1 MHz with no demodulation.
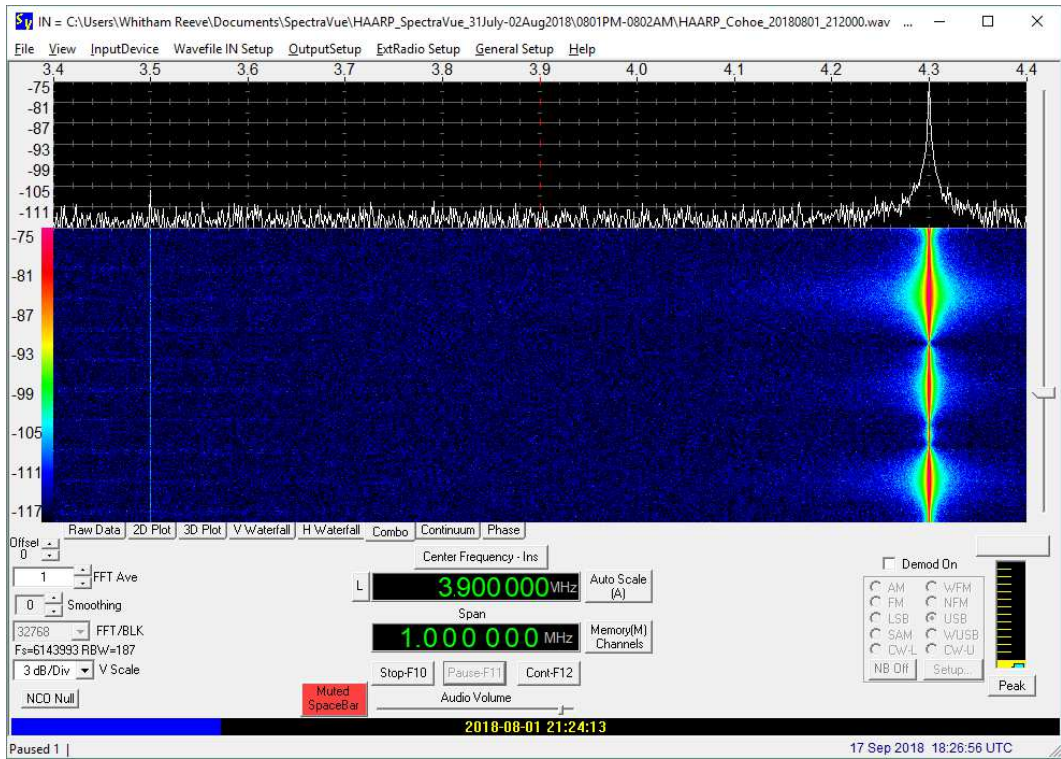
Figure 13.f ~ SpectraVue: 2124:13 UTC, 01 August, Recording: 4.300 MHz. Displayed frequency span is 1 MHz with no demodulation.
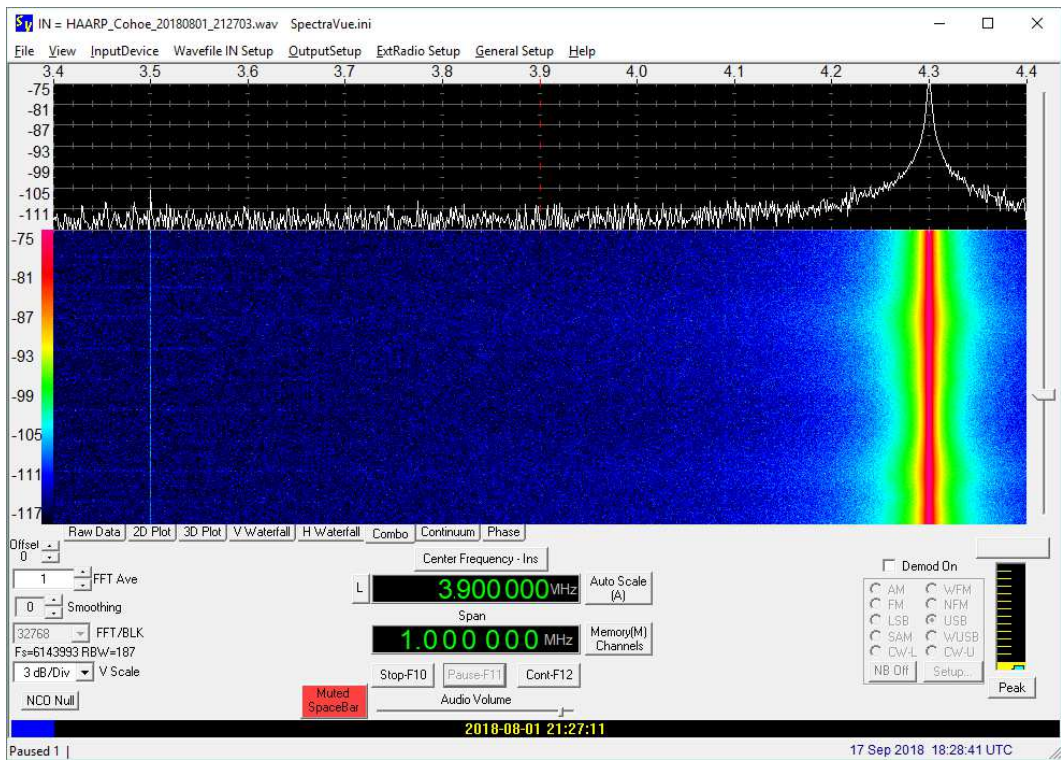
Figure 13.g ~ SpectraVue: 2127 UTC, 01 August, Recording: 4.300 MHz. Displayed frequency span is 1 MHz with no demodulation.

01 and 02 August 2018: The following twelve spectrum images show frequency modulation. The cnter frequencies and frequency span are indicated. The modulation used ±10 kHz sweep from center frequency and 50 s total duration of each sweep set. The IRI beam pointing angle was changed with each sweep set, which resulted in changed received signal level. Beam angles are unknown so I could not correlate signal levels.
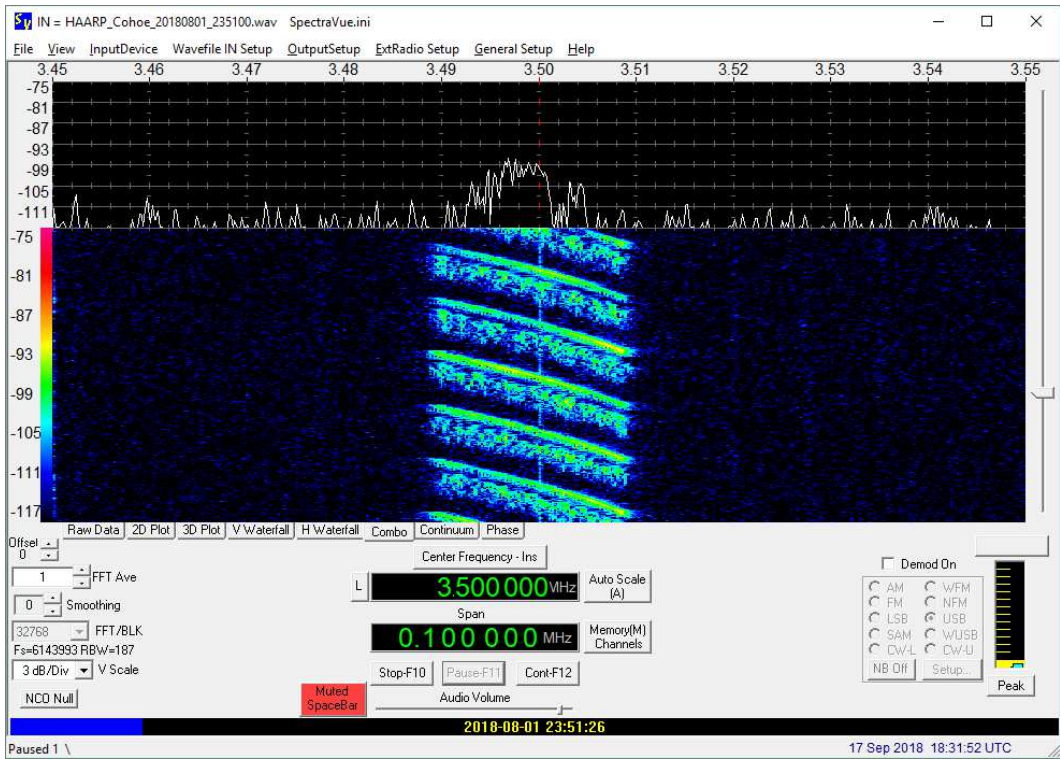
Figure 14.a ~ SpectraVue: 2151:26 UTC, 01 August, Recording: 3.500 MHz center frequency FM. Displayed frequency span is 100 kHz with no demodulation.
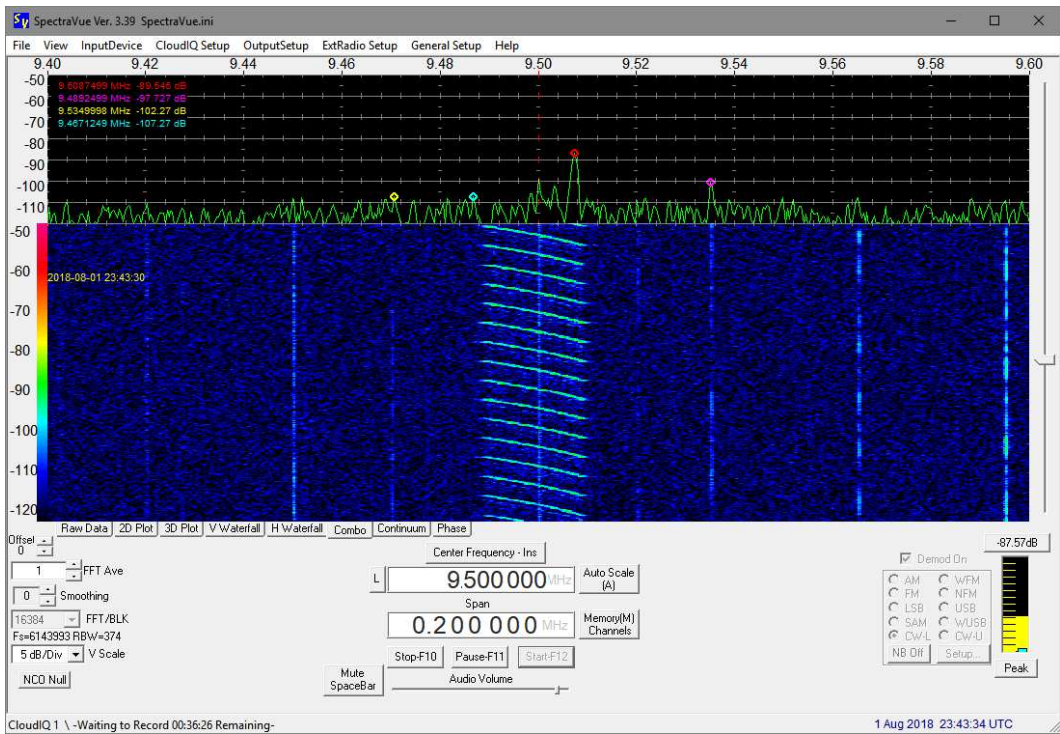
Figure 14.b ~ SpectraVue: 2343:34 UTC, 01 August, Live: 9.500 MHz center frequency FM. Displayed frequency span is 200 kHz with no demodulation.
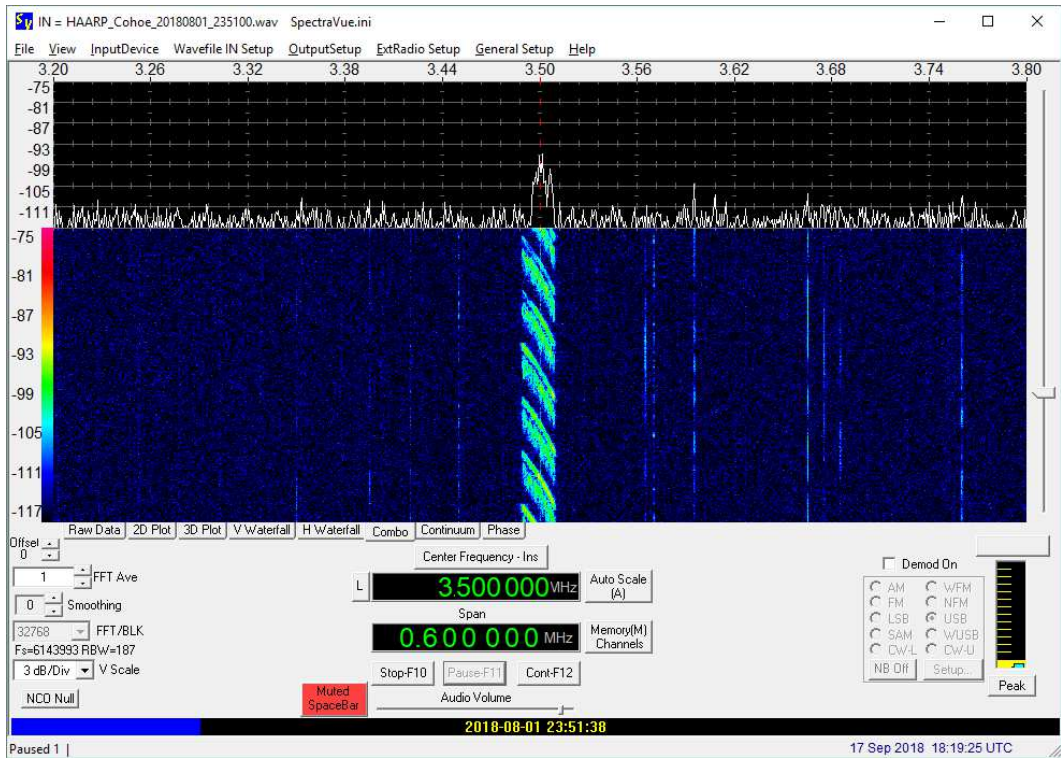
Figure 14.c ~ SpectraVue: 2351:38 UTC, 01 August, Recording: 3.500 MHz center frequency FM. Displayed frequency span is 600 kHz with no demodulation.
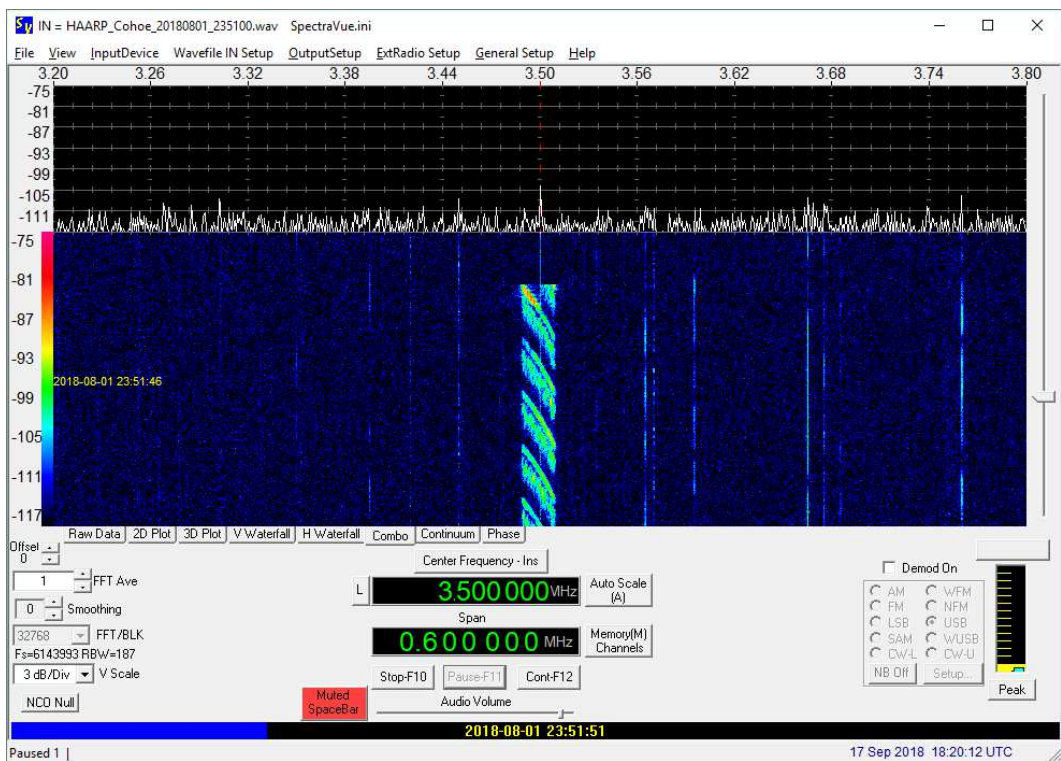
Figure 14.d ~ SpectraVue: 2351:51 UTC, 01 August, Recording: 3.500 MHz center frequency FM. Displayed frequency span is 600 kHz with no demodulation.
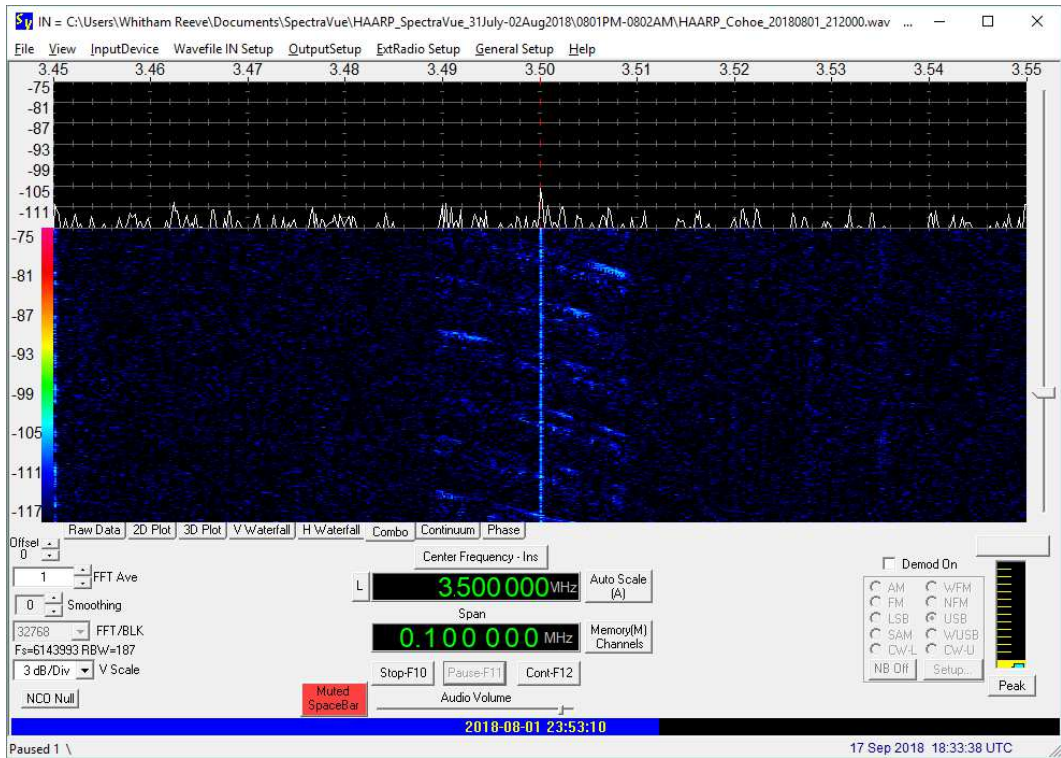
Figure 14.e ~ SpectraVue: 2353 UTC, 01 August, Recording: 3.500 MHz center frequency FM. Displayed frequency span is 100 kHz with no demodulation.
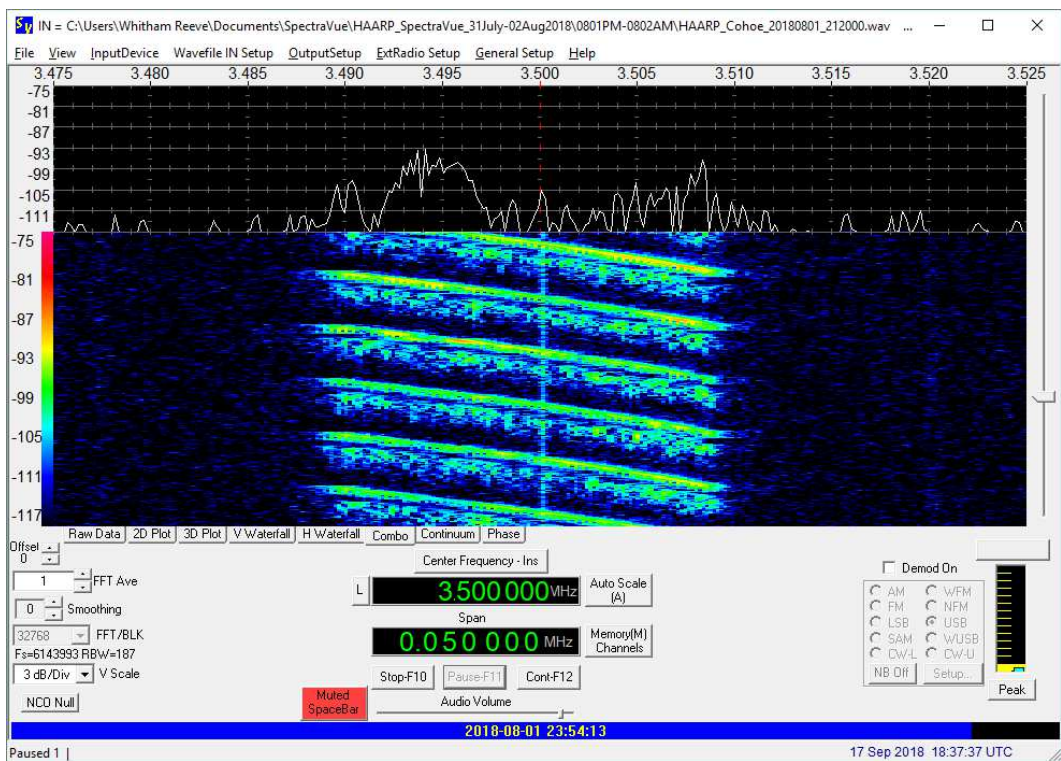
Figure 14.f ~ SpectraVue: 2354:13 UTC, 01 August, Recording: 3.500 MHz center frequency FM. Displayed frequency span is 50 kHz with no demodulation.
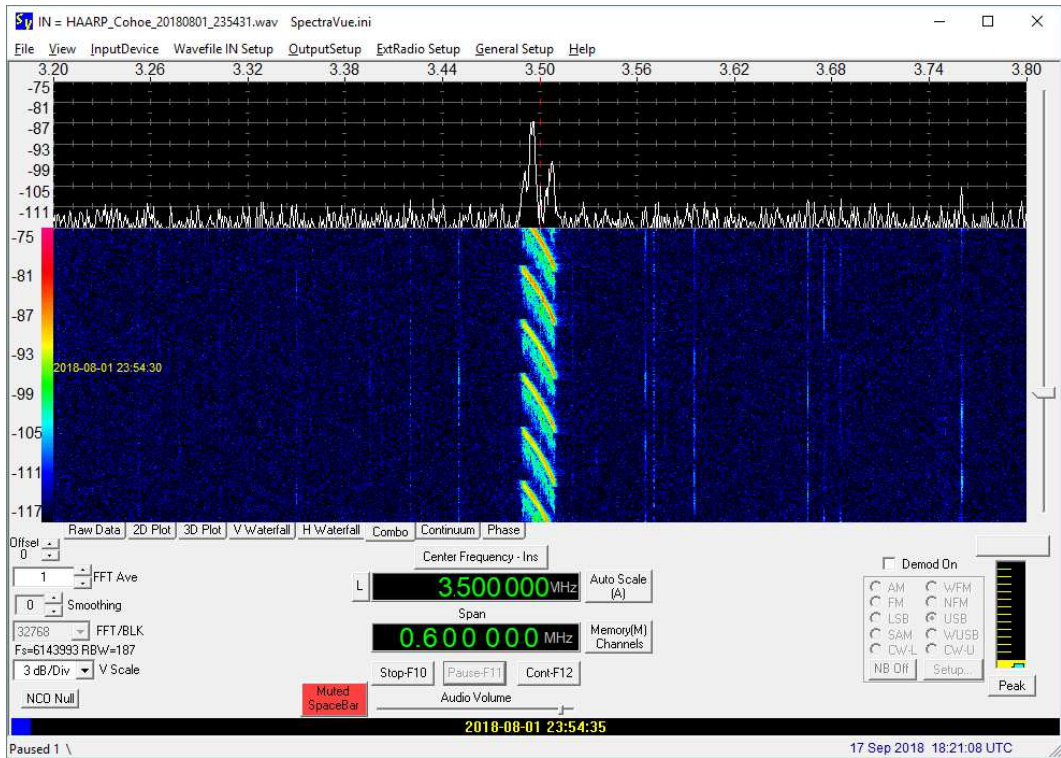
Figure 14.g ~ SpectraVue: 2354:35 UTC, 01 August, Recording: 3.500 MHz center frequency FM. Displayed frequency span is 600 kHz with no demodulation.
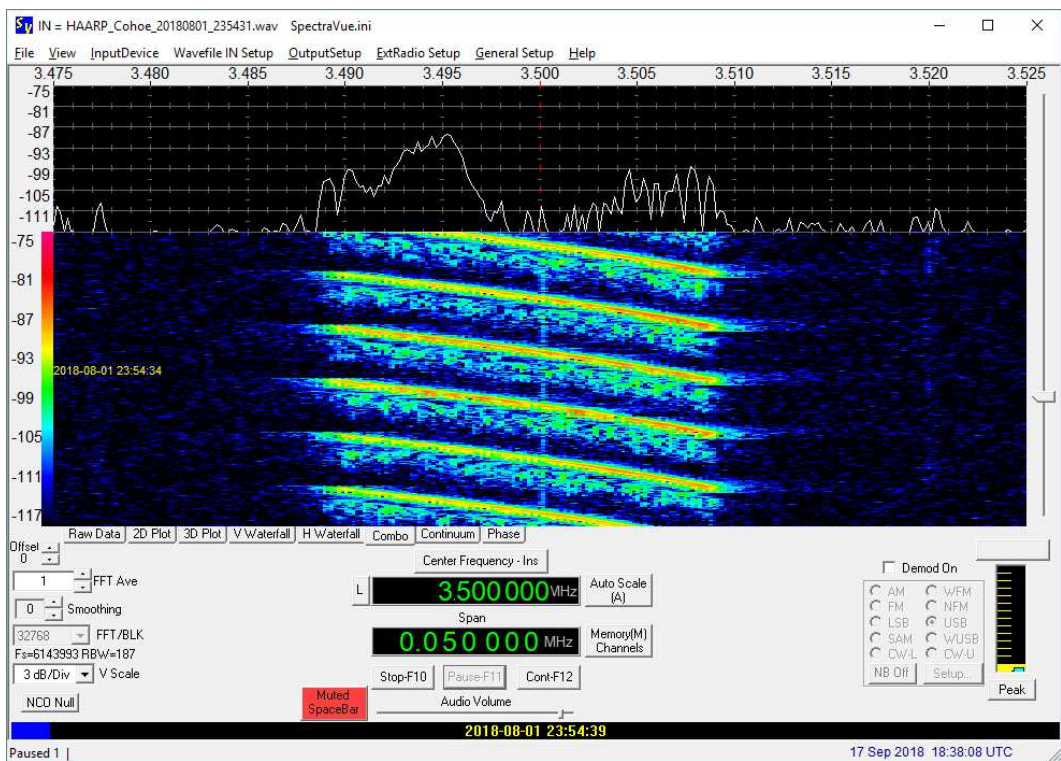
Figure 14.h ~ SpectraVue: 2354:39 UTC, 01 August, Recording: 3.500 MHz center frequency FM. Displayed frequency span is 50 kHz with no demodulation.
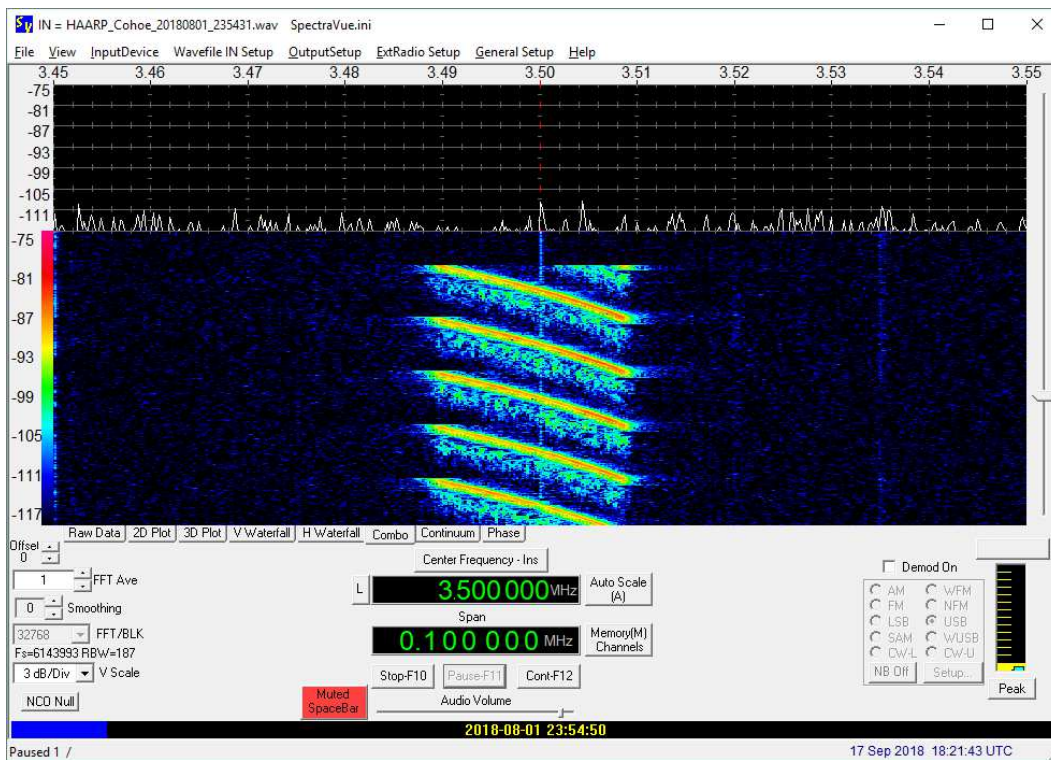
Figure 14.i ~ SpectraVue: 2354:50, 01 August, Recording: 3.500 MHz center frequency FM. Displayed frequency span is 100 kHz with no demodulation.
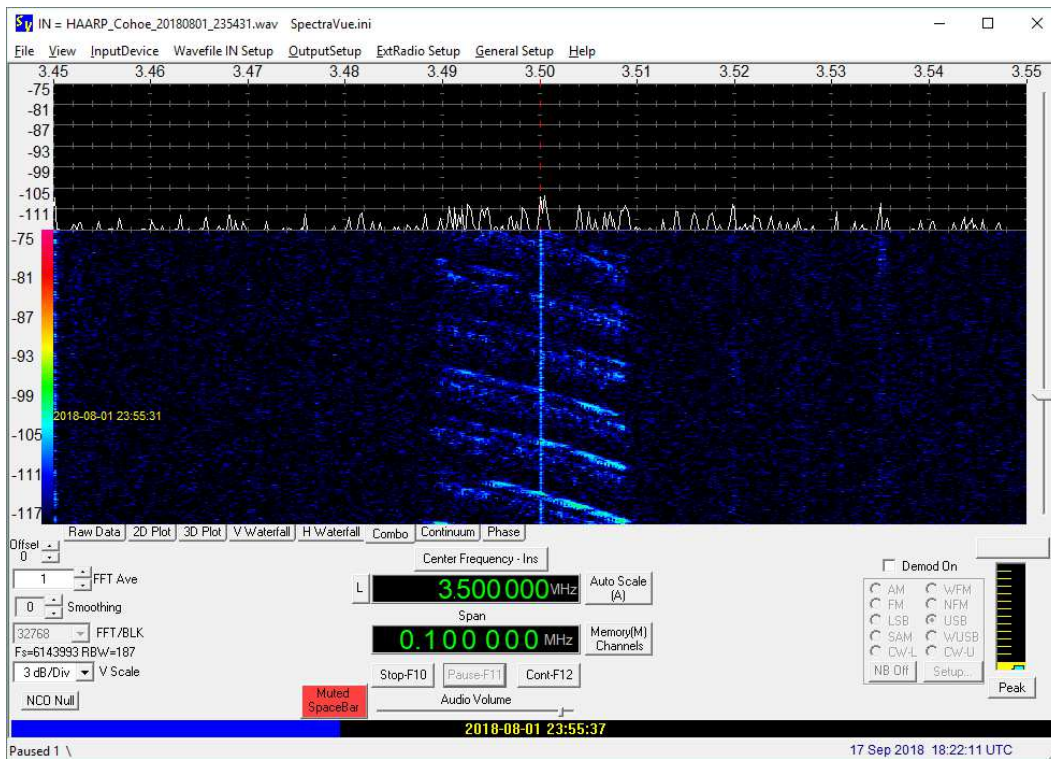
Figure 14.j ~ SpectraVue: 2355:37 UTC, 01 August, Recording: 3.500 MHz center frequency FM. Displayed frequency span is 100 kHz with no demodulation.
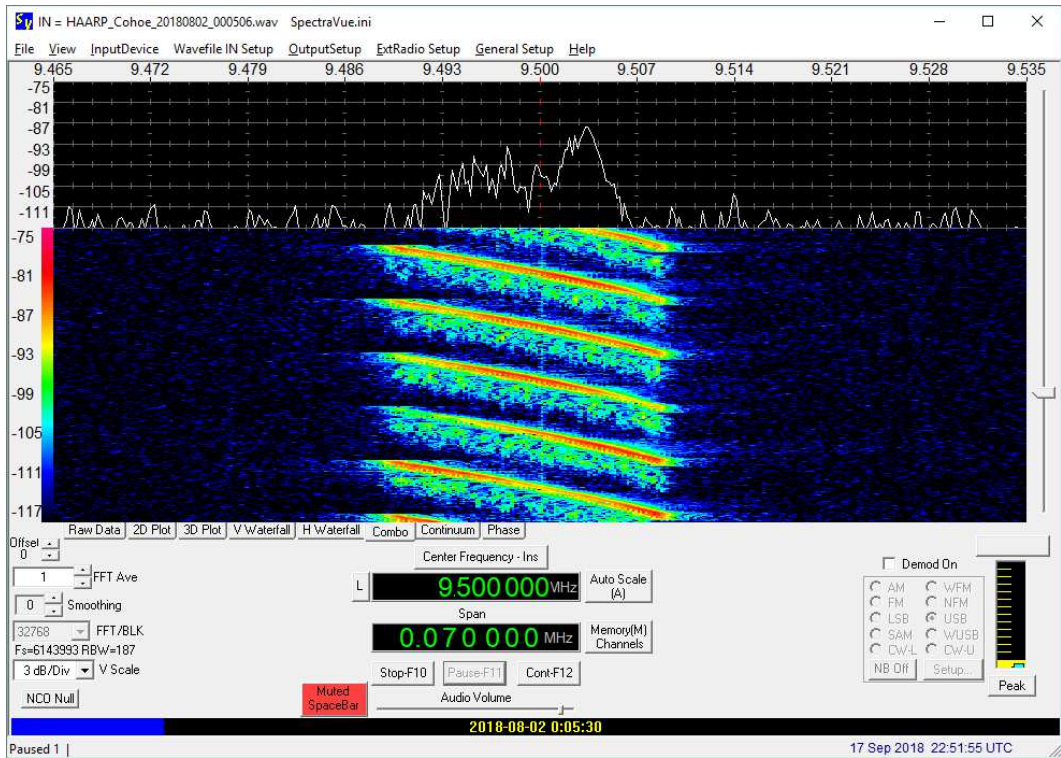
Figure 14.k ~ SpectraVue: 0005 UTC, 02 August, Recording: 9.500 MHz center frequency FM. Displayed frequency span is 70 kHz with no demodulation.
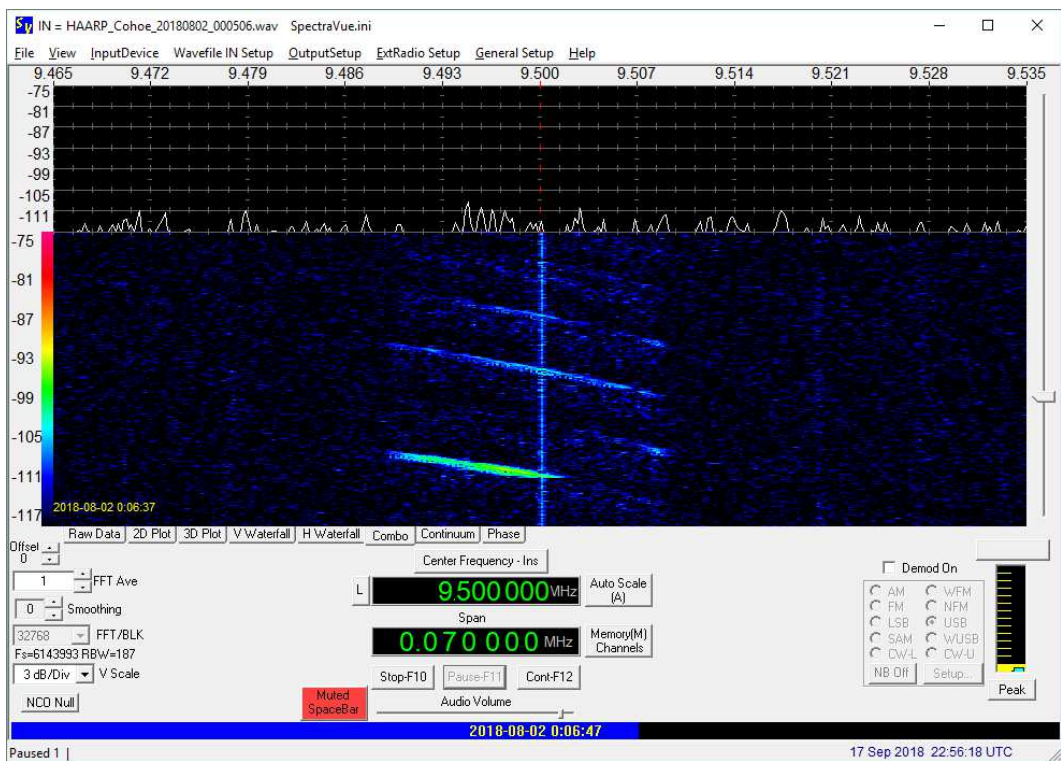
Figure 14.l ~ SpectraVue: 0006:47 UTC, 02 August, Recording: 9.500 MHz center frequency FM. Displayed frequency span is 70 kHz with no demodulation.

02 August 2018: The following are WSPR experiments in the 80 and 40 m amateur radio bands. The displayed center frequency and transmitted frequency are the same. These transmissions involved various beam pointing angles including in line with magnetic field lines and not ("low elevation").
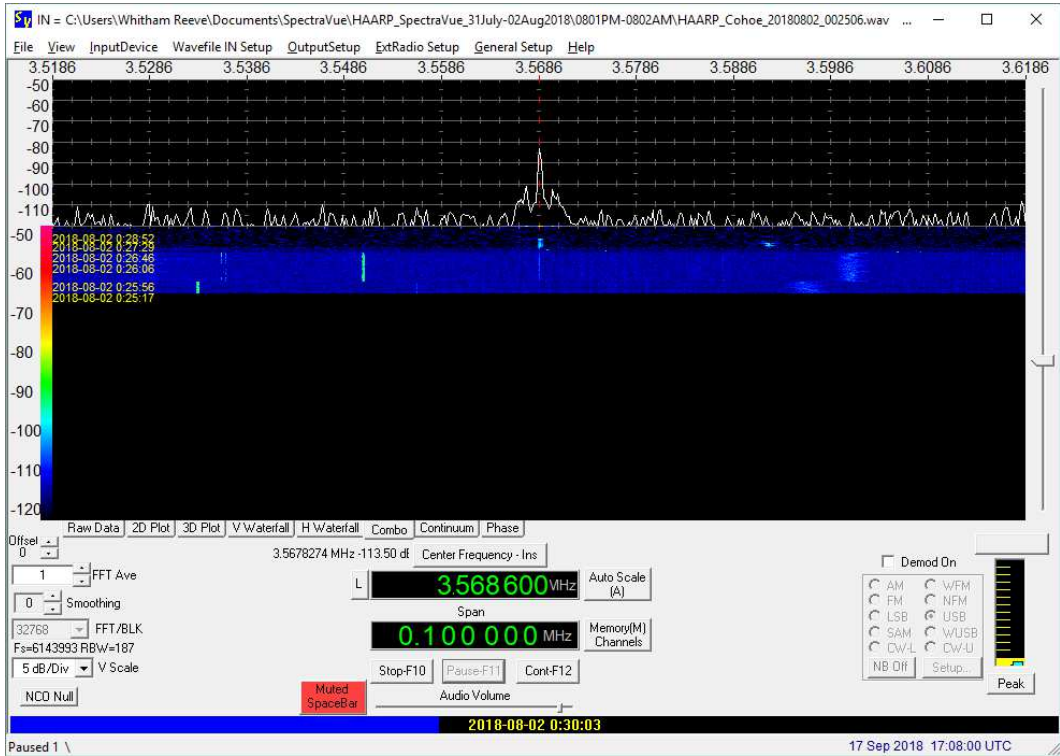
Figure 15.a ~ SpectraVue: 0030:03 UTC, 02 August, Recording: 3.5686 MHz WSPR ("low elevation"); no demodulation.
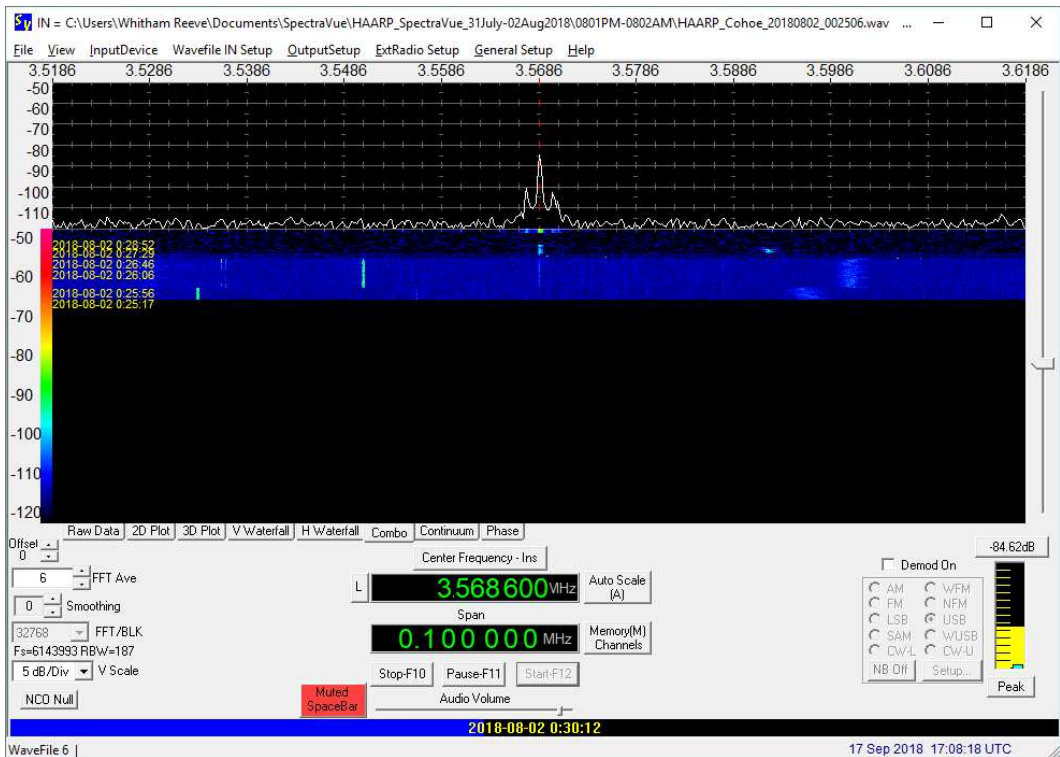
Figure 15.b ~ SpectraVue: 0030:12 UTC, 02 August, Recording: 3.5686 MHz WSPR ("low elevation"); no demodulation.
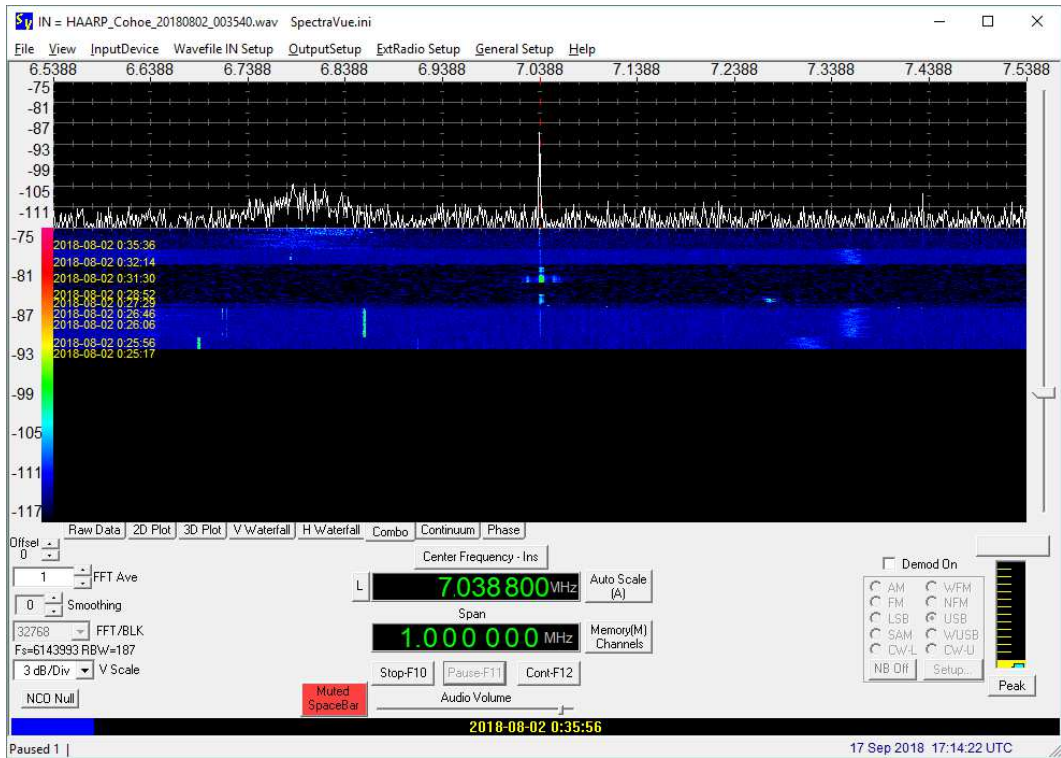
Figure 15.c ~ SpectraVue: 0035 UTC, 02 August, Recording: 7.0386 MHz WSPR ("low elevation"); no demodulation.
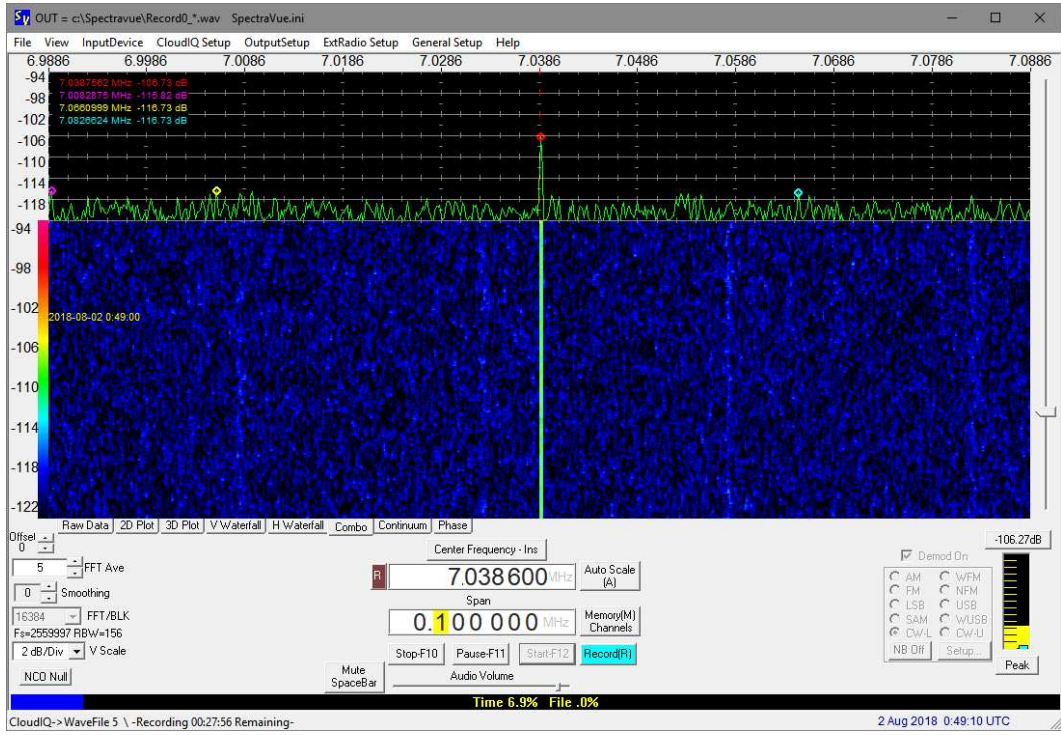
Figure 15.d ~ SpectraVue: 0049 UTC, 02 August, Live: 7.0386 MHz WSPR ("low elevation"); no demodulation.

6. Discussion

The setup used at CRO during the summer campaign was much the same as the spring campaign except that I also used the SDRPlay RSP2Pro SDR receiver and associated SDRuno software to some extent. However, I found

it difficult to set the receiver gain to provide a spectrum display comparable to the Cloud-IQ receiver and SpectraVue. The background noise is displayed differently; each receiver showed artifacts not visible on the other. The RSP2Pro showed wide noise areas centered on the receiver frequency. These could be due to high received signal levels but an overload was never indicated, and it was noted that the noise area subsided somewhat when a 30 dB attenuator was inserted at the antenna input. More investigation is required in how to setup the receiver to handle both strong and weak signals during a given transmitting session.

Another difference between the two receivers and software is the WAV file recording of the I-Q signals. SpectraVue allows multiple schedules to be setup whereas SDRuno allows only one, the latter being rather inconvenient. The signals recorded by SpectraVue are decimated, which results in a lower bit-rate being delivered to the PC.

---

7. References and Weblinks

{4NEC2}   https://www.qsl.net/4nec2/
{DTIC}   HAARP Research and Applications, 1990, Defense Technical Information Center Report
             ADA355641, available at: https://archive.org/details/DTIC_ADA355641
{GCMap}   http://www.gcmap.com/mapui?P=5KS-GKN

{Reeve16}   Reeve, W., HAARP Antenna Array ~ Photographic Tour 2016, available at:
             http://www.reeve.com/Documents/Articles%20Papers/Reeve_HAARP16.pdf
{Reeve17}   Reeve, W., HAARP Diagnostic Instruments ~ Photographic Tour 2017, available at:
             http://www.reeve.com/Documents/Articles%20Papers/Reeve_HAARP17.pdf
{Reeve18}   Reeve, W., HAARP: Radio Observations of the HAARP Research Campaign in April 2018, available
             at: http://www.reeve.com/Documents/Articles%20Papers/Reeve_HAARP_Obsv_Apr2018.pdf
{ReeveLWA}   Reeve, W., Modeling the Long Wavelength Array Crossed-Dipole Antenna, 2014, available at:
             http://www.reeve.com/Documents/Long%20Wavelength%20Array/Reeve_LWA-Model.pdf
{ReeveVLF}   Reeve, W., VLF-LF Loop Antenna Installation at Cohoe Radio Observatory, available at: To be
             published

{WSPR}   http://physics.princeton.edu/pulsar/K1JT/wspr.html
{WSPRnet}   http://wsprnet.org/drupal/

Author: Whitham Reeve is a contributing editor for the SARA journal, Radio Astronomy. He obtained B.S. and M.S. degrees in Electrical Engineering at University of Alaska Fairbanks, USA. He worked as a professional engineer and engineering firm owner/operator in the airline and telecommunications industries for more than 40 years and now manufactures electronic equipment used in radio astronomy. He has lived in Anchorage, Alaska his entire life. Email contact: whitreeve@gmail.com

Appendix ~ Reception Log

The reception log is based on WAV file recordings that are, for the most part, reconciled with tweets by the HAARP Chief Scientist. Some discrepancies are noted between tweeted times and frequencies and spectrum displays but the frequencies listed are actual. Some differences were expected due to the nature of the experiments. A question mark (?) indicates that the recording was ended before the transmissions were stopped or the signals were too weak to see.

30 July 2018: The offsets were 7, 8, 10 and 12 kHz with 2.5 min on and 0.5 min off sequence. In some cases only a single carrier channel or only three channels were received, possibly because the other channels were too weak or never transmitted.
.
4.293, 4.300, 4.307, 4.314 MHz, Δ = 7 kHz (on 21:03:00, off 2105:30)
4.292, 4.300, 4.308, 4.316 MHz, Δ = 8 kHz (on 2106:00, off 2108:30)
4.290, 4.300, 4.310, 4.320 MHz, Δ = 10 kHz (on 2109:00, off 2111:30)
4.288, 4.300, 4.312, 4.324 MHz, Δ = 12 kHz (on 2112:00, off 2114:30)
4.300 MHz (on 2115:00, off ?)
4.292, 4.300, 4.308, 4.316 MHz, Δ = 8 kHz (on 2121:00, off 2123:30)
4.290, 4.300, 4.310, 4.320 (very weak) MHz, Δ = 10 kHz (on 2124:00, off 2126:30)
4.288, 4.300, 4.312, 4.424 MHz, Δ = 12 kHz (on 2127:00, off 2129:30)
4.300 MHz (on 2130:00, off 2132:30)
4.293, 4.300, 4.307, 4.314 MHz, Δ = 7 kHz (on 2133:00, off ?)
4.300 MHz (on 2139:00?, off ?)

WSPR transmissions in the 80 m band during this session were made on an incorrect frequency.
3.5926 MHz WSPR (on 2340:00, off 2342:00)
3.5926 MHz WSPR (on 2343:59, off 2346:00)
3.5926 MHz WSPR (on 2348:00, off 2350:00) lower sideband 3.5914 MHz, upper sideband 3.5938 MHz
3.5926 MHz WSPR (on 2352:00, off 2354:00)
3.5926 MHz WSPR (on 2356:00, off 2358:00) lower sideband 3.5914 MHz, upper sideband 3.5938 MHz
3.5926 MHz WSPR (on 0000:00, off 0002:00)
7.0386 MHz WSPR (on 0004:00, off 0006:00)

31 July 2018: Both single frequencies and multi-carrier frequencies were transmitted. For the single frequency setups the step size was 10 kHz. When multi-carrier transmissions were used, the offsets were 5, 6, 7 and 8 kHz with 2.5 min on and 0.5 min off sequence.

2.750 MHz (on 2007:00, off 2008:30)
2.760 MHz (on 2009:00, off 2010:00)
2.770 MHz (on 2010:30, off 2011:30)
2.780 MHz (on 2012:00, off 2013:00)
2.790 MHz (on 2013:30, off 2014:30)
2.800 MHz (on 2015:00, off 2016:00)
2.810 MHz (on 2016:30, off ?)

4.300 MHz, (on 205?, off)

2.850 MHz, (on 21??, off 2114:30)
2.840 MHz, (on 2115:00, off 2117:30)
2.830, 2.835, 2.840, 2.845, 2.850, 2.855 MHz, Δ = 5 kHz (on 2118:00, off 2120:30)
2.828, 2.834, 2,840, 2.846, 2.852, 2.858 MHz, Δ = 6 kHz (on 2121:00, off 2123:30)
2.833, 2.840, 2,847, 2,854, 2.861 MHz, Δ = 7 kHz (on 2124:00, off 2126:30)
2.832, 2,840, 2.848, 2,856, 2.864 (very weak) MHz, Δ = 8 kHz (on 2127:00, off 2129:30)
2.840 MHz, (on 2130:00, off ?)
2.835, 2.840, 2.845, 2.850, 2.855 MHz, Δ = 5 kHz (on 2135:00, off 2135:30)
2.834, 2.840, 2.846, 2.852, 2.858 (very weak) MHz, Δ = 6 kHz (on 2136:00, off 2138:30)
2.833, 2.840, 2.847, 2.854, 2.861 (very weak) MHz, Δ = 7 kHz (on 2139:00, off 2141:30)
2.832, 2.840, 2.848, 2.856, 2.864 MHz, Δ = 8 kHz (on 2142:00, 2144:30 off)
2.840 MHz, (2145:00, off 2147:30)
2.830 (very weak), 2.835, 2.840, 2.845, 2.850 (pulsing) MHz, Δ = 5 kHz (on 2148:00, off 2150:30)
2.834, 2.840, 2.846, 2.852 MHz, Δ = 6 kHz (on 2151:00, off 2153:30)
2.833, 2.840, 2.847, 2.854 MHz, Δ = 7 kHz (on 2154:00, off 2156:30)
2.824 (very weak), 2.832, 2.840, 2.848, 2.856, 2.864, Δ = 8 kHz (very weak) MHz (on 2157:00, off 2159:30)

2.800 MHz (on 2205:05, off ?)
2.850 MHz (on 2207:05, off 2209:40)
3.025 MHz (on ?, off 2213:00)
2.750 MHz (on 2214:20, off 2216:19)
2.800 MHz (on 2217:00, off 2219:40)
2.850 MHz (on 2220:10, off 2223:00)
3.025 MHz (on ?, off 2226:19)
2.750 MHz, (on 2227:25, off 2229:40)
2.756, 2.800 MHz, (on ?, off ?)

2.850, 4.400 MHz (on 2250:00?, off 2251:30)
2.850, 4.450 MHz (on 2252:00, off 2254:30)
2.850, 4.250 MHz (on 2255:00, off 2257:30)
2.850 MHz, (on 2258:00, off 2300:30)
2.850, 4.350 MHz (on 2301:00, off 2303:30)
2.850, 4.400 MHz (on 2304:00, off 2306:30)
2.850, 4.450 MHz, (on 2307:00, off 2309:30)
2.850, 4.250 MHz (on 2310:00, off 2312:30)
2.850, 4.300 MHz (on 2313:00, off 2315:30)
2.850, 4.350 MHz (on 2316:00, off 2318:30)
2.850, 4.400 MHz (on 2319:00, off 2321:30)
2.850, 4.450 MHz (on 2322:00, off 2324:30)
2.850, 4.250 MHz (2325:00, off 2327:30)
2.850, 4.300 MHz (on 2328:00, off 2330:30)
2.850, 4.350 MHz (on 2331:00, off 2333:30)

2.850, 4.400 MHz (on 2334:00, off 2336:30)
2.850, 4.450 MHz (on 2337:00, off 2339:30)

WSPR transmissions in the 80 m band during this session were made on an incorrect frequency.
3.5926 MHz WSPR (on 2340:00, off 2342:00)
3.5926 MHz WSPR (on 2344:00, off 2346:00)
3.5926 MHz WSPR (on 2348:00, off 2350:00)
3.5926 MHz WSPR (on 2352:00, off 2354:00)
3.5926 MHz WSPR (on 2356:00, off 2358:00)
3.5926 MHz WSPR (on 0000:00, off 0002:00)
7.0386 MHz WSPR (very weak at first but no reception afterwards) (on 0004:00, off 0006:00)

01 August 2018: Most transmissions consisted of a single frequency at 4.3, 3.5 or 9.5 MHz. The 3.5 and 9.5 MHz transmissions used a sawtooth modulation (FM).

4.300 MHz (on 2000:00, off 2029:30)
4.300 MHz (on 2030:00, off 2032:00); note: 5.730 MHz not recorded
4.300 MHz (on 2033:00, off 2035:00)
4.300 MHz (on 2036:00, off 2038:00)
4.300 MHz (on 2039:00, off 2041:00)
4.300 MHz (on 2042:00, off 2044:00)
4.300 MHz (on 2045:00, off 2047:00)
4.300 MHz (on 2048:00, off 2050:00)
4.300 MHz (on 2054:00, off 2056:00)
4.300 MHz (on 2057:00, off 2059:00)

4.300 MHz (on 2121:00, off 2123:00)
4.300 MHz (on 2124:00, off 2126:00)
4.300 MHz (on 2127:00, off 2129:00)

The sweeps were ±10 kHz from center frequency with 50 s total duration of each sweep set. The IRI beam direction was changed with each sweep set resulting in changed received signal level
3.500 MHz (FM, 20 kHz deviation, 0.33 Hz sweep rate) (on 2351:00, off 2351:50)
3.500 MHz (FM, 20 kHz deviation, 0.33 Hz sweep rate) (on 2353:00, off 2353:50)
3.500 MHz (FM, 20 kHz deviation, 0.33 Hz sweep rate) (on 2354:00, off 2354:50)
3.500 MHz (FM, 20 kHz deviation, 0.33 Hz sweep rate) (on 2355:00, off 2355:50)
3.500 MHz (FM, 20 kHz deviation, 0.33 Hz sweep rate) (on 2356:00, off 2356:50)
3.500 MHz (FM, 20 kHz deviation, 0.33 Hz sweep rate) (on 2357:00, off 2357:50)

9.500 MHz (FM, 20 kHz deviation, 0.33 Hz sweep rate) (on 0000:00, off 0001:50)
9.500 MHz (FM, 20 kHz deviation, 0.33 Hz sweep rate) (on 0002:00, off 0002:50)
9.500 MHz (FM, 20 kHz deviation, 0.33 Hz sweep rate) (on 0003:00, off 0003:50)
9.500 MHz (FM, 20 kHz deviation, 0.33 Hz sweep rate) (on 0004:00, off 0004:50)
9.500 MHz (FM, 20 kHz deviation, 0.33 Hz sweep rate) (on 0005:00, off 0005:50)

9.500 MHz (FM, 20 kHz deviation, 0.33 Hz sweep rate) (on 0006:00, off 0006:50)
9.500 MHz (FM, 20 kHz deviation, 0.33 Hz sweep rate) (on 0007:00, off 0007:50)

WSPR experiments were made with IRI antennas directed toward "low elevation". The antennas in a previous session (not recorded) were directed vertically for NVIS.
3.5686 MHz WSPR (on 0025:30, off 0028:00)
3.5686 MHz WSPR (on 0030:00, off 0032:00)
7.0386 MHz WSPR (on 0034:00, off 0036:00)
7.0386 MHz WSPR (on 0038:00, off 0040:00)
7.0386 MHz WSPR (on 0042:00, off 0044:00)

Document Information

Author: Whitham D. Reeve

Copyright: ©2018, 2019 W. Reeve

Revisions: 0.0 (Original draft started, 19 Aug 2018)

0.1 (Added frequency log, 16 Sep 2018)

0.2 (Completed frequency log, 17 Sep 2018)

0.3 (Minor edits, 16 Oct 2018)

0.4 (Formatted spectrum images, 23 Oct 2018)

0.5 (Completed numbering of all figures, 26 Oct 2018)

0.6 (Added LWA antenna pattern, 27 Oct 2018)

0.7 (Added RF TLP diagram, 28, Oct 2018)

0.8 (Final edits prior to distribution, 31 Oct 2018)

0.9 (Distribution, 22 Nov 2018)

1.0 (Minor editorial improvements, 03 Mar 2019)

Word count: 6205

File size (bytes): 19129344